1988

Sample introduction techniques for inductively coupled plasma mass spectrometry

Shiuh-Jen Jiang
Iowa State University

INFORMATION TO USERS

The most advanced technology has been used to photograph and reproduce this manuscript from the microfilm master. UMI films the original text directly from the copy submitted. Thus, some dissertation copies are in typewriter face, while others may be from a computer printer.

In the unlikely event that the author did not send UMI a complete manuscript and there are missing pages, these will be noted. Also, if unauthorized copyrighted material had to be removed, a note will indicate the deletion.

Oversize materials (e.g., maps, drawings, charts) are reproduced by sectioning the original, beginning at the upper left-hand corner and continuing from left to right in equal sections with small overlaps. Each oversize page is available as one exposure on a standard 35 mm slide or as a 17″ × 23″ black and white photographic print for an additional charge.

Photographs included in the original manuscript have been reproduced xerographically in this copy. 35 mm slides or 6″ × 9″ black and white photographic prints are available for any photographs or illustrations appearing in this copy for an additional charge. Contact UMI directly to order.

Accessing the World's Information since 1938

300 North Zeeb Road, Ann Arbor, MI 48106-1346 USA

Order Number 8825931

Sample introduction techniques for inductively coupled plasma mass spectrometry

Jiang, Shiuh-Jen, Ph.D.

Iowa State University, 1988

U·M·I

300 N. Zeeb Rd.
Ann Arbor, MI 48106

PLEASE NOTE:

In all cases this material has been filmed in the best possible way from the available copy. Problems encountered with this document have been identified here with a check mark __√__.

1. Glossy photographs or pages _____
2. Colored illustrations, paper or print _____
3. Photographs with dark background _____
4. Illustrations are poor copy _____
5. Pages with black marks, not original copy _____
6. Print shows through as there is text on both sides of page _____
7. Indistinct, broken or small print on several pages __✓__
8. Print exceeds margin requirements _____
9. Tightly bound copy with print lost in spine _____
10. Computer printout pages with indistinct print _____
11. Page(s) _____ lacking when material received, and not available from school or author.
12. Page(s) _____ seem to be missing in numbering only as text follows.
13. Two pages numbered _____. Text follows.
14. Curling and wrinkled pages _____
15. Dissertation contains pages with print at a slant, filmed as received __✓__
16. Other _____

_____

_____

Sample introduction techniques

for

inductively coupled plasma mass spectrometry

by

Shiuh-Jen Jiang

A Dissertation Submitted to the

Graduate Faculty in Partial Fulfillment of the

Requirements for the Degree of

DOCTOR OF PHILOSOPHY

Department: Chemistry

Major: Analytical Chemistry

Approved:

Signature was redacted for privacy.

In Charge of Major Work

Signature was redacted for privacy.

For the Major Department

Signature was redacted for privacy.

For the Graduate College

Iowa State University
Ames, Iowa

1988

PREFACE

Inductively coupled plasma mass spectrometry (ICP-MS) is a new technique for elemental and isotopic analysis that combines the remarkable characteristics of the ICP for atomizing and ionizing injected samples with the sensitivity and selectivity of mass spectrometry. To date, most publications have focused on either the basic fundamental principles of the technique or on specific applications. Only a few publications have dealt with sample introduction for ICP-MS. There are several well known approaches to introducing samples into an ICP, and some of these have now been tried for ICP-MS.

Most applications of ICP-MS to date have employed a conventional pneumatic nebulizer for the introduction of solution samples. However, there are many potential applications for elemental analysis in which time or solubility constraints render sample dissolution inconvenient. Furthermore, the sample dissolution step can always increase the risk of contamination. For these reasons it is desirable to investigate the suitability of ICP-MS for providing analytical measurements with other types of sample introduction techniques.

The primary advantages of liquid chromatographic (LC) sample introduction over continuous sample introduction are the following. First, instead of determining the sample's total element content, LC sample introduction permits elemental speciation measurements. Second, LC sample introduction can separate potential interferents from the analyte elements before they reach the plasma. Third, LC sample

introduction can preconcentrate the elements of interest before they are introduced into the ICP. Fourth, LC sample introduction requires only a small volume of sample. Fifth, because of the transient nature of the signal, LC (or more correctly flow injection) sample introduction only requires a short wash out time.

Despite these advantages, there is relatively little widespread use of chromatography in ICP atomic spectroscopy. The basic criteria for a successful LC-ICP study are efficient interface performance and good enough detection limits for analysis of real samples. In LC-ICP-MS studies, the sample introduction system acts as the interface between the chromatograph and the spectrometer. Developments in the interface may hold the key to the success or failure of the whole approach.

It is the overall purpose of this thesis to study the suitability of various sample introduction techniques for ICP-MS.

The format of this thesis is divided into five sections. Each section stands alone as a complete manuscript with figures, tables and literature cited all numbered in consecutive order within each section.

The first section of this thesis describes arc nebulization for elemental analysis of conducting solids by ICP-MS. The sample serves as a cathode in an intermittent arc. The eroded sample material condenses into particulates which are then transported into an ICP with detection of the resulting ions by a mass spectrometer. The resulting analyte spectra consist almost entirely of atomic ions with little or no detectable oxide ions. Polyatomic ions from acid solvents (e.g., ClO^+), which interfere with some analyte peaks during aqueous nebulization, are also avoided. Detection limits are in the $\mu g\ g^{-1}$ range for the elements

studied. Calibration curves are linear up to ~ 0.1 wt % analyte; curvature is seen at higher concentrations for some elements. Samples can be changed in 1 min, and relative precision and accuracy are approximately 5%.

A technique for direct elemental and isotopic analysis of powders is described in section two. A powdered sample is mixed with graphite and pressed into a conducting pellet. The pellet is eroded by an intermittent arc, and the resulting sample particles are injected into an ICP-MS. This provides rapid survey analysis and determination of elemental and isotope ratios without dissolution of the sample. Small peaks for ArC^+, ArO^+ and Ar_2^+ are the only species detected in the background spectrum above m/z = 45. The absence of nebulized water effectively suppresses formation of metal oxide ions. Detection limits are 30 - 50 $\mu g\ g^{-1}$ for the elements studied. Isotope ratios may be determined with a precision of approximately 1% relative standard deviation for major constituents. Various rare earth elements are determined quantitatively at 0.1-1% levels in the original sample.

Two important problems currently facing ICP-MS users are matrix effects and spectral interferences. Spectral interferences result from mass overlap between analyte ions and concomitant (or polyatomic) ions. In addition to overlap problems, the analyte sensitivity can also depend on the total solute concentration of the sample solution. This phenomenon has been called a matrix effect.

A procedure for removal of some interferences from Mo and Ti for the measurement of Cd, Zn and Cu in ICP-MS is described in section three. Complexes of Mo (VI) or Ti (IV) with N-methylfurohydroxamic acid (N-

MFHA) are retained on a column packed with polystyrene divinylbenzene. At the pH values chosen, Cu, Zn and Cd wash rapidly through the column and are detected by ICP-MS without interference from metal oxide ions of Ti or Mo. Detection limits are 1 to 2 $\mu g\ g^{-1}$, and analyte recoveries are essentially 100%. The resin capacity for the Ti and Mo complexes is sufficient for several hundred injections, and the complexes can be readily washed from the column with 1 M HNO_3 in methanol. Separation techniques are also of potential value for isotope ratio determinations, in which all the isotopes of interest should be free of overlap interference. Isotope ratios for Cu, Zn, and Cd have been determined on eluting peaks without interference from metal oxide ions of Ti or Mo.

U (VI) also forms a stable complex with N-MFHA, and matrix effects caused by excess U can be avoided by chromatographic removal of the U complex. Various other potentially interfering elements with aqueous oxidation states +4 or higher (e.g., Sn, W, Hf or Zr) could also be separated by this technique.

Element "speciation" measurements, the identification and quantitation of the individual chemical forms of an element, are toxicologically and biochemically important. In section four, we demonstrate that ICP-MS is a sensitive and elemental selective detector for LC.

Anionic compounds containing phosphorous or sulfur are separated by reverse phase LC with tetraalkylammonium salts as ion pairing reagents. Phosphorous and sulfur in the separated compounds are detected on line as $^{31}P^+$ or $^{34}S^+$ by ICP-MS. Inorganic phosphates and nucleotides are separated with detection limits of 0.4-4 ng P. These detection limits

are superior by several orders of magnitude to those reported for phosphorous detection by atomic emission spectrometry (AES). Sulfur compounds studied include inorganic sulfates and amino acids; detection limits are ~ 7 ng S and are comparable or superior to previous results for AES detection. In general, the analyte sensitivity decreases as the concentration of organic modifier (methanol or acetonitrile) in the mobile phase increases. Therefore, the chromatographic conditions are designed to minimize the concentration of organic modifier necessary.

Because of the intense background peaks from Ar^+ and ArH^+, the use of ICP-MS for potassium isotope measurements (m/z = 39, 40, and 41) has not been reported. Section five of this thesis demonstrates that Ar^+ and ArH^+ ions from an Ar ICP can be attenuated drastically simply by adjusting the plasma operating conditions. Positioning the sampling orifice relatively far from the load coil combined with use of low forward power and high aerosol gas flow rate causes the background mass spectrum to become dominated by NO^+. Nearly all the Ar^+ and ArH^+ ions are suppressed under these conditions, which frees m/z = 39 and 41 for potassium isotope ratio measurements. The precision is 0.3 - 0.9% relative standard deviation for potassium concentrations in the range 1 - 50 mg L^{-1}. The determined ratios are ~ 9% higher than the accepted value and also vary with the concentration of sodium concomitant, so calibrations and chemical separations are desirable. These observations should permit use of ICP-MS for rapid isotope ratio determinations of potassium from humans or other biological organisms.

SECTION I.

ARC NEBULIZATION FOR ELEMENTAL ANALYSIS OF CONDUCTING SOLIDS BY INDUCTIVELY COUPLED PLASMA MASS SPECTROMETRY

INTRODUCTION

Inductively coupled plasma mass spectrometry (ICP-MS) is a rapidly growing technique for multielemental analysis. The attractive features of ICP-MS include excellent detection limits, inherently simple spectra, and similar sensitivity for most elements (1-3). Nearly all the published research in ICP-MS reported so far has described results obtained during nebulization of aqueous samples. This approach to sample introduction has the desirable features that a homogeneous analytical sample is easily obtained, external standards are easily prepared, and internal standardization or isotope dilution is straightforward. However, there are many potential applications for elemental analysis in which time or solubility constraints render sample dissolution inconvenient. Furthermore, mineral acids can yield undesirable molecular peaks such as ClO^+ or SO^+ in the background mass spectra obtained from the ICP (2,3). For these reasons, it is desirable to investigate the suitability of ICP-MS for providing analytical measurements with other types of sample introduction techniques.

Various methods for introducing solids directly into ICPs for atomic emission spectrometry (AES) have been described (4), none of which have found very widespread application in the analytical community. Gray has studied a laser ablation technique for introducing solids into an ICP with subsequent detection by MS (5), and Gray and Date have briefly described some work with electrothermal vaporization of solids and ICP-MS (6). In these studies, the experimental variables used to generate mobile particles from the sample are isolated from those used for

atomization and ionization in the ICP so that these processes can be independently optimized. This concept of separating sampling and ionization is also incorporated into the present work, in which an arc nebulization technique is used to analyze solids by ICP-MS. Although this nebulization technique is limited to conducting matrices, there is still considerable use for it as indicated by the countless analyses done routinely in the metals industry by arc or spark emission spectrometry.

EXPERIMENTAL SECTION

Solids Nebulizer

Prior use of this nebulization device in conjunction with optical spectroscopic measurements has been described in publications by Jones et al. (7) and Winge et al. (8); neither of these workers used this nebulizer with an ICP. The nebulizer is illustrated in Figure 1. The sample serves as the cathode and is sealed on the top of the arc chamber via the O-ring depicted. The arc is generated between the Cu anode and the sample cathode. The arc erodes material from the sample into the Ar flow. The arc is intermittent at a frequency of approximately 1 MHz (7) and "wanders" about the exposed cathode surface so that a representative section is sampled. For the steels used in this study the sample material was removed at a rate of approximately 1 mg min^{-1}. The sample must have a flat, solid surface large enough to seal onto the O-ring; otherwise, no special sample preparation procedure is necessary. The voltage and current parameters used were similar to those described in ref. 8.

The eroded material forms particulates that are carried by the Ar flow through a plastic tube (2 m long x 3 mm i.d.) into the axial channel of the ICP. Previous publications indicate that the particles are 1-3 μm in diameter and that the nebulizer can be considerably further from the plasma (i.e., at least 20 m) if desired without serious transport loss of sample (7,8). Some sample material does condense in the sample transport tubing as noted previously. The arc can be

Table 1. Experimental parameters

Outer gas flow rate	17 L min^{-1}
Auxiliary gas flow rate	0.5 L min^{-1}
Aerosol gas flow rate	0.6 L min^{-1}
Forward power	1.1 kW
Sampling position	10 mm from load coil on center
Sampling orifice diameter	0.63 mm

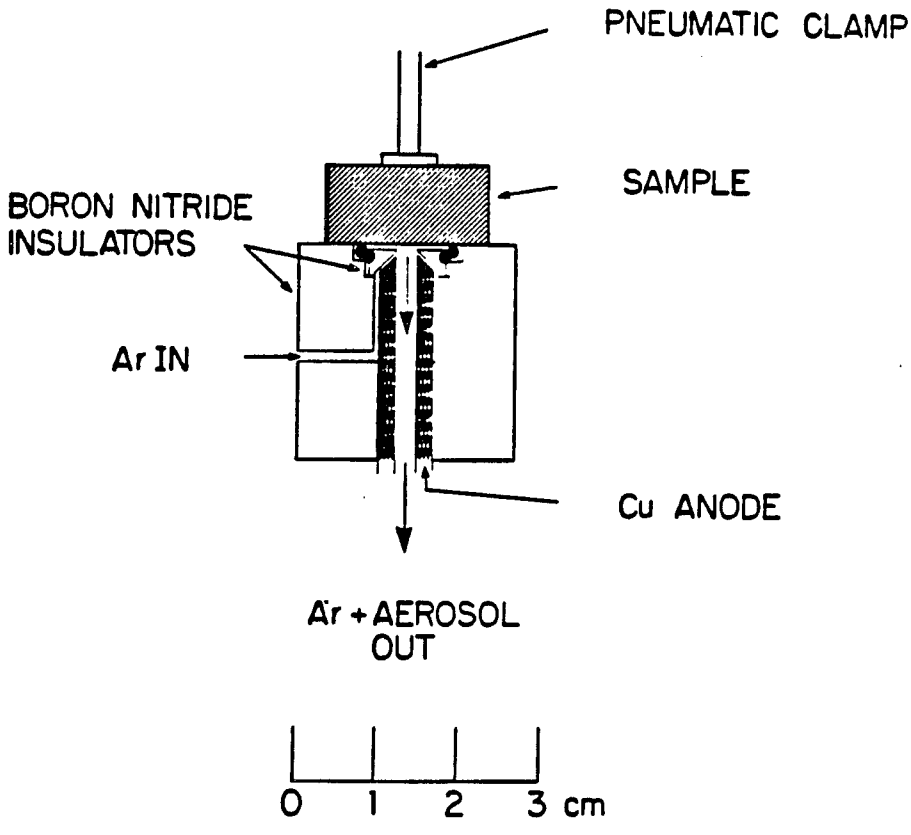

Figure 1. Scale diagram of arc nebulizer

operated continuously for approximately 2 min before the O-ring degrades thermally. In order to remove contaminants from the sample surface the arc was operated for 10-15 s before analytical data were obtained.

ICP-MS Instrumentation

The device used was assembled in the Ames Laboratory and has been described previously (9). Relative to commercial ICP-MS devices this homemade instrument tends to have comparable or better sensitivity (i.e., slope of calibration curve) but higher background and poorer detection limits. Operating conditions are listed in Table 1. The ICP and ion optical parameters were optimized by first maximizing the signal for background ions with a sample in place and aerosol carrier gas flowing through the nebulizer and ICP but with the nebulizing arc off. The same ion optical settings provided optimum ion transmission when the arc was initiated and sample particles were flowing into the plasma. Resolution and dc bias voltage on the quadrupole rods were selected to resolve adjacent peaks without undue discrimination against ions at higher m/z values. Data were obtained either by selected ion monitoring at a single m/z value for the duration of the arc cycle or by repetitive scanning over a selected m/z range with signal averaging. In the repetitive scanning mode each sweep of the selected m/z range was done in 0.08 s; i.e., 20 μs was spent on each of 4096 channels in the memory of the signal averager. Typically 256 such sweeps were obtained and summed to yield one of the spectra shown below. The resulting data were then stored on floppy disk. The electron multiplier was operated in a

pulse counting mode.

Standards and Calibration

Specimens of steel standard reference materials (SRMs) whose elemental composition was certified by the National Bureau of Standards were used. The integrated background signal at a m/z value void of a peak was the same whether the arc was on or off. Therefore, the background was evaluated with the arc off. In the selected ion monitoring mode the net count rate was evaluated by averaging successive 20-s integrations and subtracting the background count rate at the m/z value of interest. In the repetitive scanning mode the net count rate was evaluated by subtracting the background from the count rate at the top of the peak of interest. This could be done either after the gross count rate data were obtained or by simply stripping the background spectrum from the sample spectrum using the signal averager. The sensitivity was similar (i.e., within a factor of 2) from day to day. Thus, the sensitivity for a given element is not identical in all the figures and tables because the data were taken on various days.

RESULTS AND DISCUSSION

Selection of Operating Conditions

Numerous workers have shown that the mass spectra and analytical performance obtained from an ICP-MS device depend strongly on the operating conditions chosen. Aerosol gas flow rate is the most critical parameter for virtually all such instruments (9-11). The dependence of the net analyte signal on aerosol gas flow rate for the arc nebulizer is shown in Figure 2. Highest signal was obtained at a relatively high flow rate (~ 1 L min^{-1}), which is also generally the case for aqueous nebulization. However, the sampling orifice of the mass spectrometer tended to plug rapidly if this aerosol gas flow rate was used during arc nebulization. Therefore, a lower flow rate (0.6 L min^{-1}) was selected to permit repeated analyses while minimizing solid deposition on the orifice. At this lower flow rate the arc could be operated repeatedly for at least 3 h without noticeable clogging of the sampling orifice. An analogous compromise is also often necessary in ICP-MS with aqueous solutions; generally, operating conditions that yield the best sensitivity and detection limits also yield the worst interferences (12,13). Finally, studies of the dependence of analyte signal on sampling position indicated that the sampling position denoted in Table 1 was optimum, or nearly so, for the elements and samples studied and gas flow rate chosen.

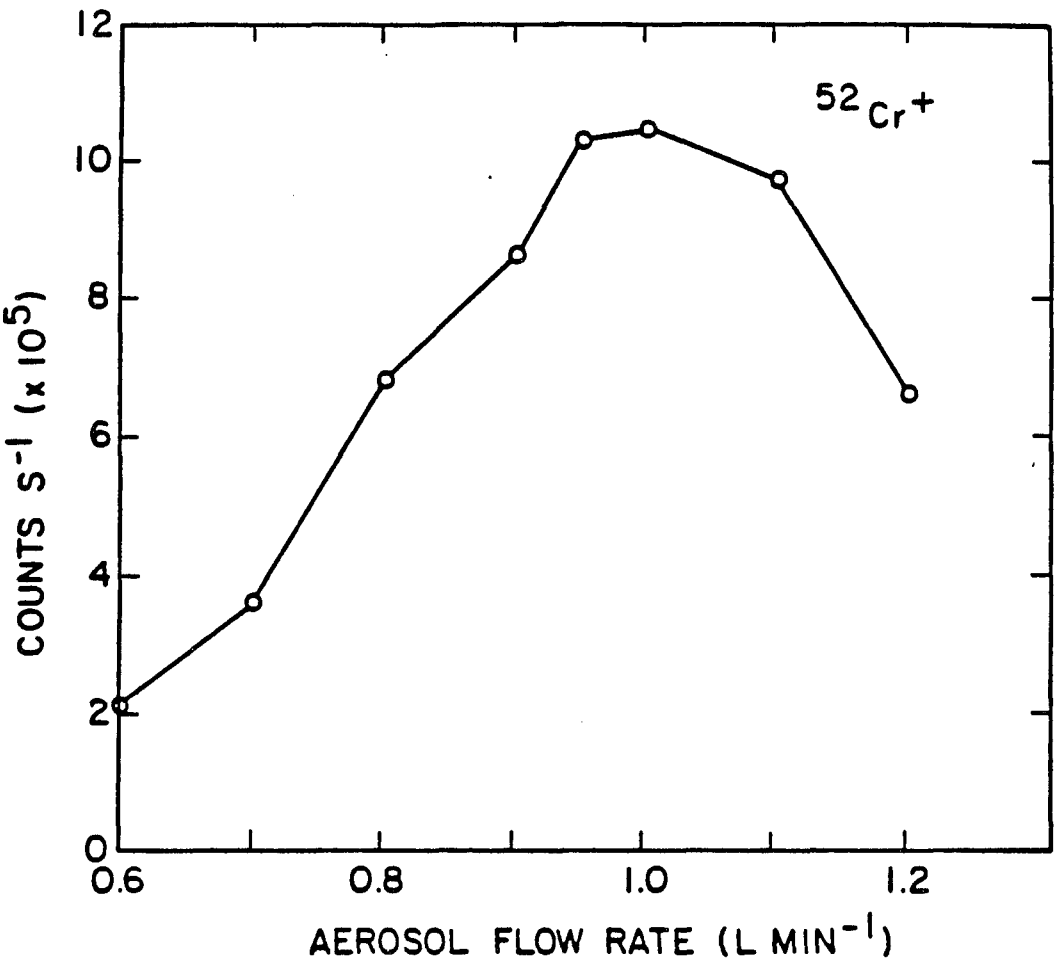

Figure 2. Dependence of net signal for $^{52}Cr^+$ on aerosol gas flow rate

Mass Spectra

The background spectrum obtained with the arc off is shown in Figure 3. The peaks for Ar^+ and ArH^+ were split because the high count rates caused pulse pileup and loss. Ar^+ was always the dominant ion, as expected from a "dry" plasma such as this. Significant peaks from O^+, OH^+, H_2O^+, NO^+, O_2^+, m/z 28 (N_2^+ and/or CO^+), and Ar_2^+ were also observed. Relative to Ar^+ the count rates for the peaks containing O and H were considerably less than during aqueous nebulization. Furthermore, the count rates for these peaks varied when argon supply tanks were changed indicating that these ions arose largely from impurities in the argon. The background spectrum in the range m/z 50-60 was considerably cleaner than when nebulized aqueous solutions (particularly ones containing concentrated mineral acids) were introduced. Gray has noted similar background spectra in his laser ablation experiments (5).

Several spectra obtained during introduction of nebulized steel particles are shown in Figures 4-6. Figure 4 was taken immediately after Figure 3, so these two spectra are comparable directly. In Figure 4, B^+ and Al^+ were clearly evident, and the signals for C^+, O^+, and N^+ were higher than in the background spectrum. The increased signal at m/z 28 was probably due to Si^+ from the sample although small amounts of Fe^{2+}, CO^+, and N_2^+ could also contribute. P^+ and S^+ could also be observed although they were not abundant in this sample. Other work in our laboratory has shown that H can be determined as ArH^+ (14). These spectra at low m/z indicated that nonmetallic impurities can potentially

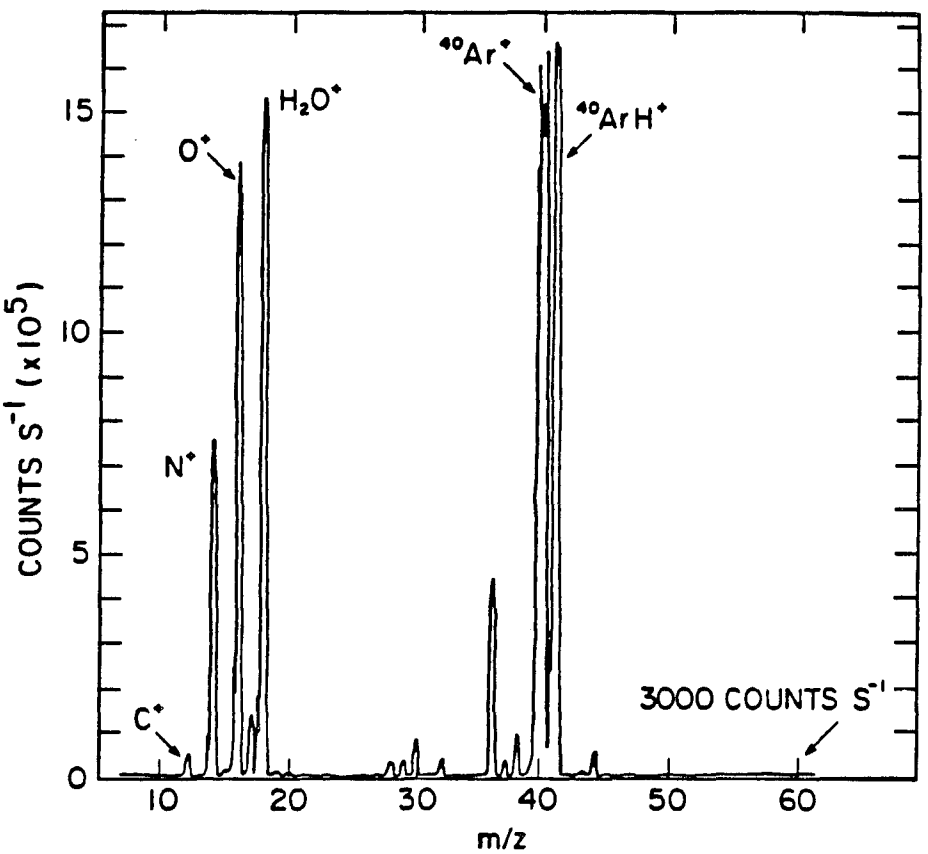

Figure 3. Background mass spectrum with arc off. This spectrum and subsequent ones were signal averaged for 256 sweeps

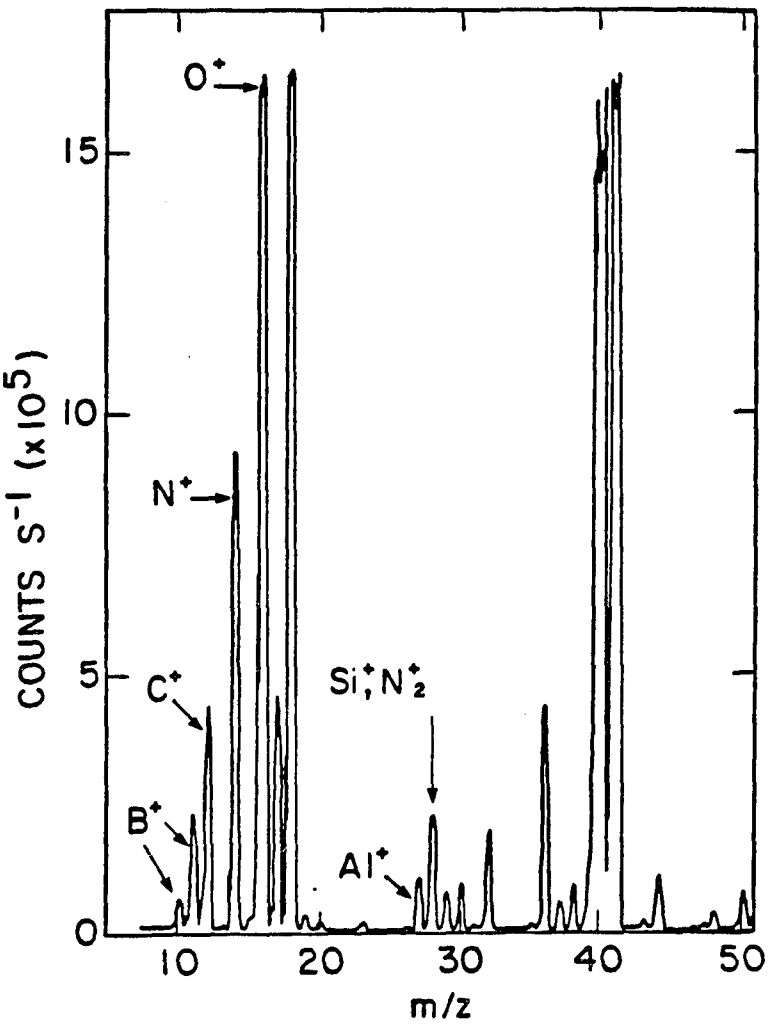

Figure 4. Spectrum of low-mass elements obtained during arcing of steel SRM 1468 (0.042% Al, 0.26% C, 0.009% B). The background count rate in this and subsequent figures is 3000 counts s^{-1}

be determined in metals by this technique, particularly if the background levels of C, N, O, and H can be reduced by purifying the argon.

A steel spectrum in the m/z range near the major sample constituent (Fe) is shown in Figure 5. The nebulizer generated enough sample particles for counting loss to be observed on the Fe^+ peaks. Nevertheless, only two potential analyte m/z values (54 and 58) were directly obscured by Fe^+. The mass analyzer used in this work permitted better resolution of $^{55}Mn^+$ and $^{53}Cr^+$ from Fe^+ than shown in Figure 5 but only at the expense of discrimination against higher m/z ions. Alloying constituents such as Ti, V, Cr, Ni, and Co were readily identified. The Cu^+ observed came solely from the metal specimen and not from the anode of the nebulizer. No MO^+ peaks were observed for Ti or V above the standard deviation of the background (~ 100 counts s^{-1}) despite the refractory nature of oxide species of these elements. The only isotope of As^+ is seen at m/z = 75 without interference from $^{40}Ar^{35}Cl^+$, which is a nuisance during nebulization of HCl or $HClO_4$ solutions.

A steel spectrum at higher m/z range is shown in Figure 6. Zr, Mo, and Nb were readily observed. Again, no detectable oxide ions were observed even though these elements form very refractory oxides (15). Although not shown in these figures, spectra from volatile elemental constituents like Ag, Sn, and Zn can be readily obtained without evidence of condensation or other loss during transport to the ICP.

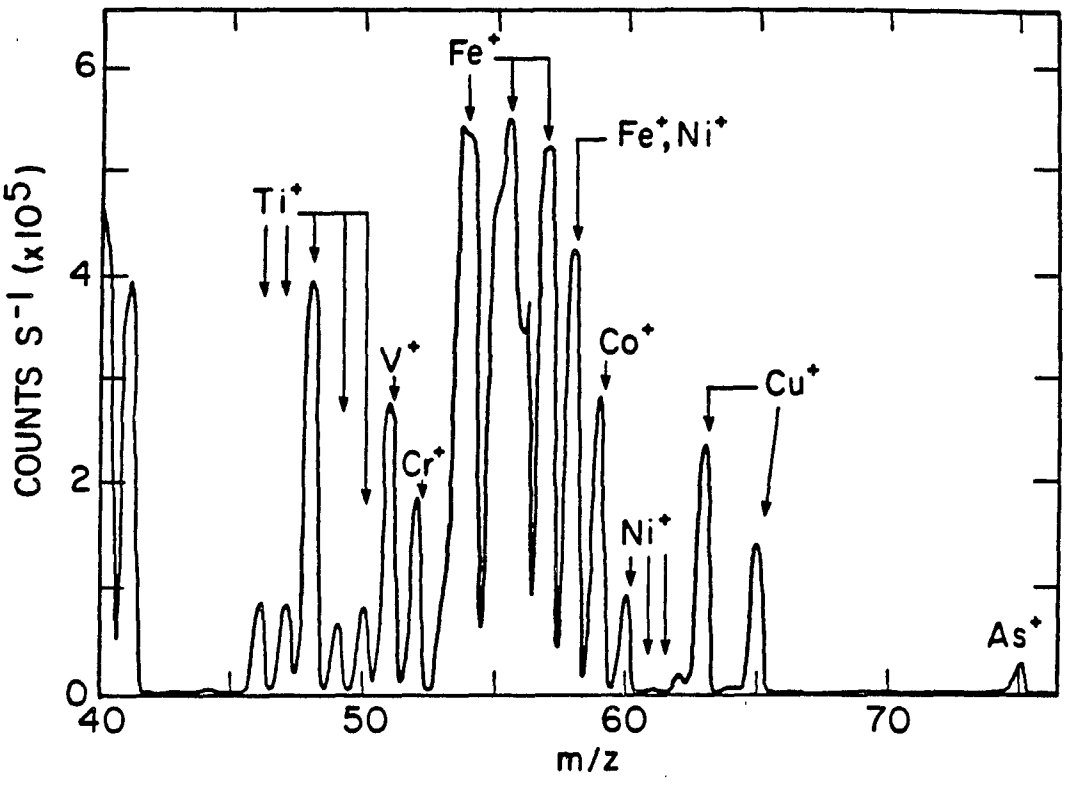

Figure 5. Spectrum of first-row transition elements obtained during arcing of SRM 1264 (0.052% As, 0.15% Co)

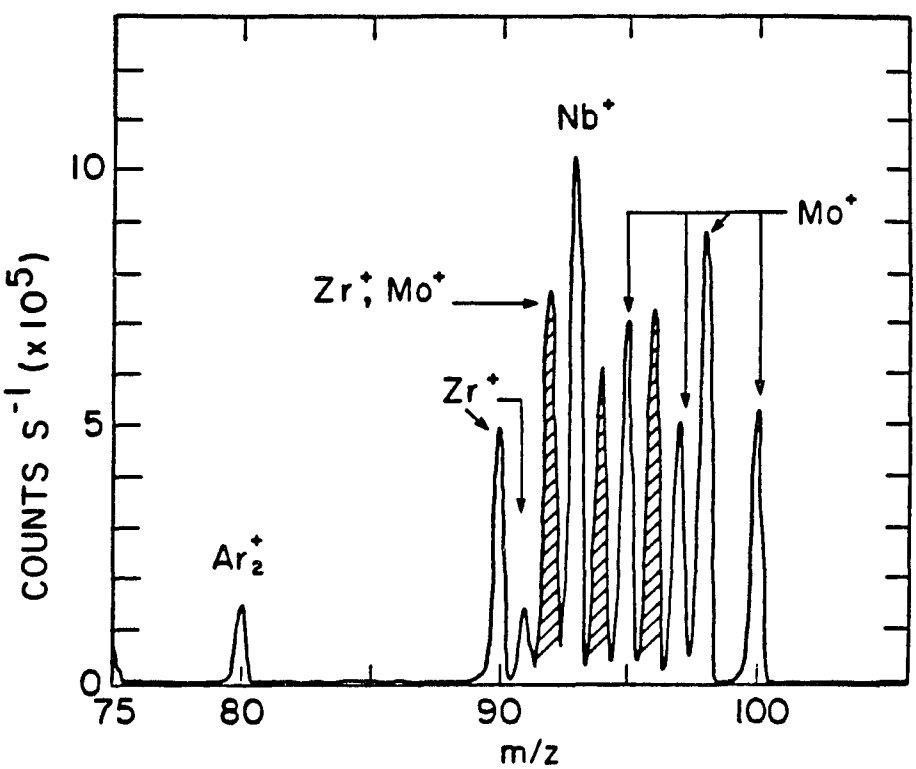

Figure 6. Spectrum of Zr, Nb, and Mo from SRM 1264 (0.157% Nb, 0.49% Mo)

Precision and Sample Cleanout Characteristics

A plot of signal for $^{52}Cr^{+}$ as a function of time is shown in Figure 7. This figure was obtained with the mass analyzer transmitting only m/z = 52 and was characteristic of those observed for other elements. The arc was turned on and off at the times denoted in the caption. The sample species reached the ICP only a few seconds after the arc was initiated. The signal rapidly attained a fluctuating steady state in which the peak-to-peak variation was approximately 10% of the signal. For the two nebulization pulses shown in Figure 7 the relative standard deviation of successive 20-s integrations was 3.3% for the first cycle and 4.4% for the second. The average count rates for the two nebulization pulses in Figure 7 differed by 3%. This latter value was representative of the average count rate for five or so successive nebulization pulses. Similar values for precision were obtained in the optical studies with this nebulizer (7,8) indicating that these values probably represented the inherent reproducibility of the nebulization process.

After the arc was extinguished the signal for Cr decayed to 1% of its maximum in 10 s and to 0.1% in 30 s. This "rinse out" time, which represented the time necessary for the aerosol gas flow to sweep the nebulizer chamber and transport tubing clear of sample particles, was rapid enough for analysis of a new sample within 1 min after nebulization of its predecessor. If necessary, the cleanout time could be decreased further by using a high Ar flow rate from a separate flow control device to sweep out the nebulizer while switching the resulting

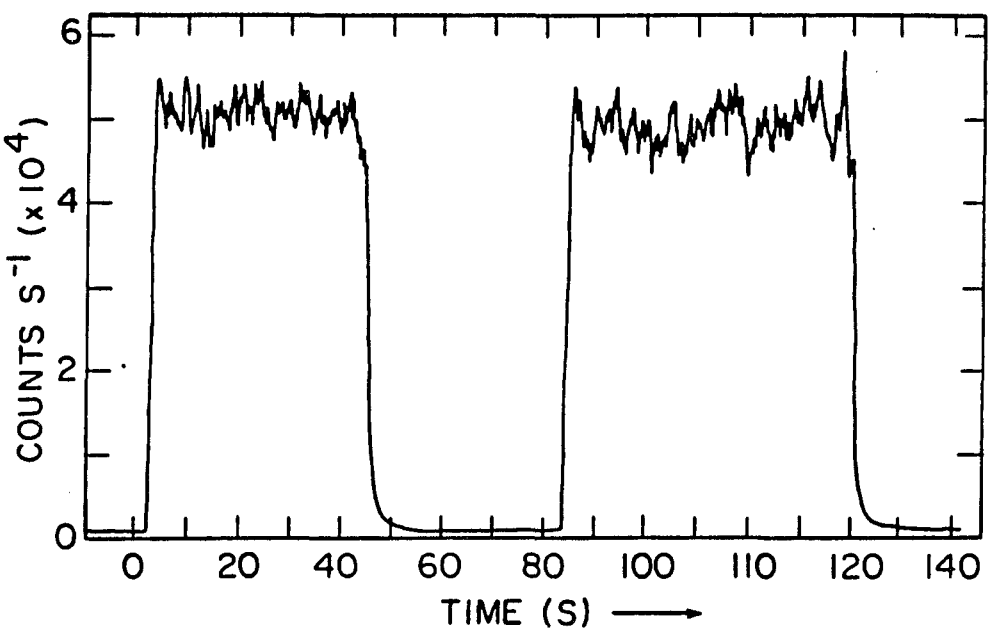

Figure 7. Count rate data for Cr^+ (SRM 1164, 0.078% Cr) as a function of time for two separate nebulization cycles, selected ion monitoring at m/z 52. The arc was turned on at 0 s, off at 45 s, on again at 80 s, and off at 118 s

gas so that it does not pass through the ICP (5). It is interesting to note that the high level of Fe in these samples and the limited temporal duration and fluctuating nature of the nebulization cycle would render ICP atomic emission spectrometry with this sample introduction device prone to spectral interference and background correction problems.

Detection Limits, Sensitivity, and Calibration Curves

Data for calibration curves, detection limits, and sensitivity were obtained in the selected ion monitoring mode. The detection limit was estimated to be the analyte concentration necessary to give a net count rate equivalent to 3 times the standard deviation of the background at the m/z value of interest. The detection limits listed in Table 2 are denoted as estimated values because the available SRMs generally were not certified at analyte concentrations near the detection limit. In other words, the detection limits determined in this study were extrapolated from count rate data obtained at concentrations considerably above the detection limit. The detection limits were in the range 0.4-4 $\mu g\ g^{-1}$ for the elements studied except Ni, which showed consistently poorer detection limits and sensitivity than other elements. Nonetheless, these data indicated the combination of arc nebulization with ICP-MS to be potentially capable of verifying the presence or absence of constituents in the microgram per gram range.

The sensitivities shown in Table 2 represented the slopes of the calibration curves at low analyte concentrations. Again, Ni showed

Table 2. Sensitivities and detection limits

Element	Isotopic abundance, %	Sensitivity, (counts s^{-1})(μg g^{-1})$^{-1}$	Detection limit, μg g^{-1}
^{27}Al	100	190	2
^{28}Si	92.2	130	6
^{48}Ti	74.0	130	2
^{51}V	99.7	240	1
^{52}Cr	83.8	220	1
^{59}Co	100	200	2
^{60}Ni[a]	26.2	21	10
^{75}As	100	76	4
^{90}Zr	51.5	370	0.8
^{93}Nb	100	790	0.4
^{98}Mo	23.7	83	4
^{120}Sn	33.0	300	1
^{181}Ta	99.9	650	0.5
^{184}W	30.6	160	2

[a] ^{58}Ni overlaps ^{58}Fe.

consistently low sensitivity. Some variation in sensitivity was observed among the other elements; the extent of this variation is greater than can be accounted for by the different isotopic abundances of the elemental peaks monitored or by m/z discrimination of the mass analyzer used. This phenomenon can be discerned by dividing the sensitivity values in Table 2 by isotopic abundance and comparing the resulting corrected values for elements of similar atomic weight and ionization energy. For example, similar sensitivity was observed for V, Cr, and Co but that for Ti was only approximately half that of the others. Likewise, the sensitivity was similar for Zr and Nb but that for Mo was poorer. It was possible that the arc nebulizer removed some elements more efficiently than others. Previous reports did not find evidence for preferential nebulization of different elements, but considerably higher aerosol gas flow rates were used than in the present work (7,8). There is at least one alternate explanation for the differing sensitivity, which is described below.

The sensitivities shown in Table 2 are much less than those obtained with this ICP-MS instrument during nebulization of aqueous solutions. To compare these figures of merit, it is instructive to first compare the nebulization rate of the two sample introduction techniques using Co as a typical analyte element. The arc nebulizer removes sample at a rate of 1 mg min^{-1}, most of this material being Fe. A trace constituent at 1 μg g^{-1} in the sample is nebulized at a rate of 1 ng min^{-1}. The ultrasonic nebulizer normally used with this ICP-MS instrument is 10% efficient at a typical uptake rate of 2 mL min^{-1}. Cobalt present at 1 mg L^{-1} in solution is transformed into aerosol at a rate of

approximately 200 ng min^{-1}, i.e., over 2 orders of magnitude faster than with the arc nebulizer.

Another possible reason for the poorer sensitivity with the arc nebulizer is the high rate of introduction of matrix element. For the figures quoted above Fe is nebulized at a rate of approximately 1 mg min^{-1}. Introduction of Fe at a similar rate for solution nebulization would require an Fe concentration of 5000 mg L^{-1}. This level of Fe would be expected to suppress analyte signals in ICP-MS of solutions (16). In fact, evidence for such suppression is apparent from the spectra in Figures 3 and 5. The peaks from the matrix element (Fe, Figure 5) are significant relative to the sum of the background ions (Figure 3) even though counting losses are occurring for the various species. The observation of comparable count rates for matrix and background ions has been identified previously as a symptom of matrix effects (16). The extent of such signal suppression need not be the same for all elements, so this effect could also contribute to the element-to-element differences in sensitivity noted above. The precise nature of matrix interferences in ICP-MS is presently uncertain as somewhat different behavior has been reported for various instruments, interferent elements, analyte elements, and operating conditions (16-20).

Despite these limitations, net analyte count rates were evaluated for a variety of steel SRMs by selected ion monitoring for each element of interest. The resulting calibration curves were linear (correlation coefficient > 0.995) for the analyte elements studied at concentrations

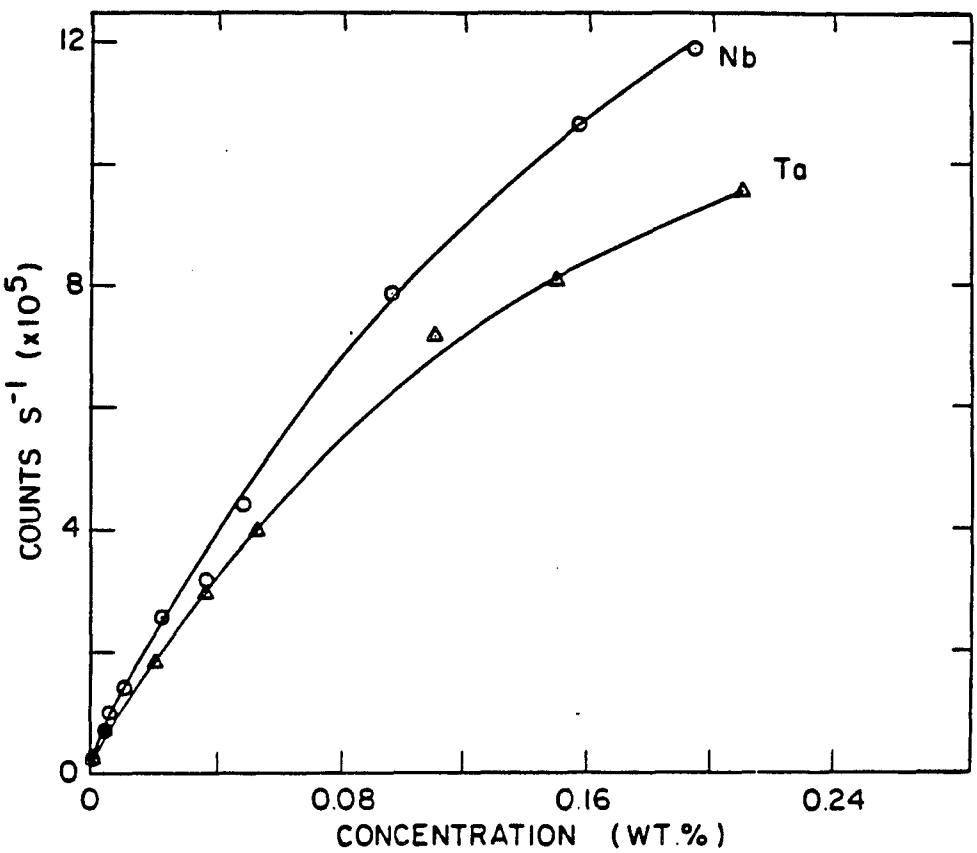

Figure 8. Calibration curves for ^{93}Nb and ^{181}Ta; data were obtained by selected ion monitoring for the indicated element

Table 3. Analysis of steel SRMs in selected ion monitoring mode[a]

	^{28}Si		^{48}Ti		^{59}Co		^{60}Ni	
SRM	det[b]	cert[c]	det	cert	det	cert	det	cert
1161	0.045	0.047	0.009	0.01	-[d]	0.26	-[d]	1.73
1162	0.280	0.28[f]	0.037	0.037	0.111	0.11	-[d]	0.70
1163	-[d]	0.41	0.011	0.01	-[d]	0.013	0.392	0.39
1164	-[d]	0.48	0.003	0.004[e]	0.026	0.028[e]	0.136	0.135
1165	0.023	0.029	-[d]	0.2	-[d]	0.008	-[d]	0.026[e]
1166	0.024	0.025	0.057	0.057[f]	-[d]	0.046	0.043	0.051
1167	0.251	0.26	-[d]	0.26	0.082	0.074	0.092	0.088
1168	0.087	0.075	0.010	0.011	0.158	0.16[f]	-[d]	1.03
2A1261	0.225	0.223	0.026	0.02	0.032	0.032	-[d]	1.99
2A1262	-[d]	0.40	-[d]	0.084	-[d]	0.30	0.586	0.60[f]
2A1263	-[d]	0.74	0.046	0.05	0.045	0.048	0.313	0.32
2A1264	0.079	0.066	-[d]	0.23	0.148	0.15	0.193	0.192
2A1265	-[d]	0.008[e]	-[d]	0.0006	-[d]	0.007	0.033	0.041

[a]Concentrations are listed in weight percent.

[b]Determined.

[c]Certified.

[d]Element was either outside the linear range or was not determined in this standard.

[e]Least concentrated standard used.

[f]Upper end of linear range.

^{93}Nb		^{98}Mo		^{120}Sn		^{184}W	
det	cert	det	cert	det	cert	det	cert
0.011	0.011	-[d]	0.30	0.024	0.022	0.009	0.012[e]
0.096	0.096[f]	0.080	0.080	0.066	0.066[f]	0.055	0.053
-[d]	0.195	0.116	0.12[f]	0.014	0.013	0.106	0.105
0.034	0.037	0.032	0.029	0.042	0.043	0.021	0.022
-[d]	-[d]	-[d]	0.005	-[d]	0.001	-[d]	-[d]
-[d]	0.005[e]	0.011	0.011[e]	0.003	0.005[e]	-[d]	-[d]
-[d]	0.29	0.019	0.021	-[d]	0.1	0.199	0.20[f]
0.005	0.006	-[d]	0.2	0.008	0.009	0.083	0.077
0.026	0.022	-[d]	0.19	0.012	0.011	0.017	0.017
-[d]	0.3	0.075	0.07	0.016	0.016	-[d]	0.21
0.050	0.049	0.032	0.03	-[d]	0.095	0.046	0.046
-[d]	0.157	-[d]	0.49	-[d]	0.005	0.098	0.102
-[d]	-[d]	-[d]	0.005	-[d]	0.0002	-[d]	-[d]

ranging from the minimum certified (generally ~ 0.001%) up to at least 0.1% for most elements. Analytical results for typical elements are listed in Table 3, in which the determined values were derived from a straight line fit (by least squares) to the calibration data in the indicated range. In this linear portion the individual data points were generally within ± 5% relative of the calibration line; an occasional point deviated by ± 10-20%. Comparison of the determined and certified values in Table 3 indicates that elemental constituents of steels can be determined with reasonable accuracy by arc nebulization with ICP-MS. Nickel can be determined readily above 0.05% even though the sensitivity is poorer than for other elements as noted above.

Calibration curves continued to be linear at higher concentrations for some elements, whereas calibration plots for other elements "drooped" like those shown in Figure 8. The count rates were not sufficiently high for counting loss to be the major cause of curvature. Again, it was possible that either or both the nebulization efficiency or the extent of ionization suppression changed as the analyte concentrations approached major constituent levels. It is interesting to note that Jones et al. observed similar curvature in their calibration plots for elements present above approximately 1%. They nevertheless stated that "... matrix and interelement effects ... are either not detectable or very low compared with those in conventional [i.e., non-ICP] discharges" (7). Furthermore, some other discharge-based techniques for introducing solids into ICPs also yielded calibration plots that curve at high analyte concentrations (21). The calibration curves obtained in the present work indicated that elemental

response should be calibrated with standard materials that match the samples of interest in major element composition and that bracket the analyte concentrations at both low and high ends. There are numerous analytical scenarios (e.g., process control in the metals industry) where such standards already exist or where the large numbers of analyses to be done justifies the effort to prepare solid standard materials. The calibration points in Figure 8 are close enough to the curve to indicate that analysis could be done with reasonable accuracy at concentrations above 0.1% despite the curvature noted in some of the calibration plots.

LITERATURE CITED

1. Douglas, D. J.; Houk, R. S. Prog. Anal. At. Spectrosc. 1985, 8, 1.
2. Houk, R. S. Anal. Chem. 1986, 58, 97A.
3. Gray, A. L. Spectrochim. Acta, 1985, 40B, 1525.
4. Browner, R. F.; Boorn, A. W. Anal. Chem. 1984, 56, 786A.
5. Gray, A. L. Analyst, 1985, 110, 551.
6. Gray, A. L.; Date, A. R. Analyst, 1983, 108, 1033.
7. Jones, J. E.; Dahlquist, R. L.; Hoyt, R. E. Appl. Spectrosc. 1971, 25, 628.
8. Winge, R. K.; Fassel, V. A.; Kniseley, R. N. Appl. Spectrosc. 1971, 25, 636.
9. Olivares, J. A.; Houk, R. S. Anal. Chem. 1985, 57, 2674.
10. Olivares, J. A.; Houk, R. S. Appl. Spectrosc. 1985, 39, 1070.
11. Horlick, G.; Tan, S. H.; Vaughan, M. A.; Rose, C. A. Spectrochim. Acta, 1985, 40B, 1555.
12. Douglas, D. J. unpublished data, Sciex, Inc., Thornhill, Ontario, 1985.
13. Thompson, J. J. Ph.D. Dissertation, Iowa State University, Ames, Iowa, 1986.
14. Chong, N. S. M.S. Thesis, Iowa State University, Ames, Iowa, 1985.
15. McLeod, C.; Date, A. R.; Cheung, Y. Y. Spectrochim. Acta, 1986, 41B 169.
16. Olivares, J. A.; Houk, R. S. Anal. Chem. 1986, 58, 20.
17. Tan, S. H.; Horlick, G. J. Anal. Atomic Spectrom. 1987, 2, 745.
18. Gillson, G. R.; Douglas, D. J.; Fulford, J. E.; Halligan, K. W.;

Tanner, S. D. Anal. Chem. 1988, accepted.

19. Gray, A. L. Spectrochim. Acta, 1986, 41B, 151.

20. Crain, J. S.; Houk, R. S.; Smith, F. G. Spectrochim. Acta, Part B submitted.

21. Human, H. G. C.; Scott, R. H.; Oakes, A. R.; West, C. D. Analyst, 1976, 101, 265.

SECTION II.

ELEMENTAL AND ISOTOPIC ANALYSIS OF POWDERS BY INDUCTIVELY COUPLED PLASMA MASS SPECTROMETRY WITH ARC NEBULIZATION

INTRODUCTION

Inductively coupled plasmas (ICPs) are remarkably effective media for vaporizing, atomizing and ionizing injected sample constituents for subsequent spectroscopic measurements. Samples are generally introduced into ICPs as aerosols of aqueous solutions; however, numerous sample types and applications exist for which dissolution is slow, difficult, or inconvenient. For these reasons, considerable activity is underway to analyze solids directly by ICP emission spectrometry without prior dissolution. The recent proliferation of ICP mass spectrometers (ICP-MS) has further stimulated efforts for direct elemental analysis of solids because of the sensitivity, selectivity and isotope ratio capabilities of mass spectrometric measurements (1-3). Furthermore, introduction of samples without concomitant water can attenuate some interfering background ions from the mass spectrum, particularly if dissolution requires $HClO_4$ or H_2SO_4 (1,2,4). Solid introduction techniques used with ICP-MS to date include laser ablation (5,6), electrothermal vaporization (6,7), and direct insertion of a wire loop containing the sample into the ICP (8). An arc nebulizer capable of generating aerosol particles from conducting solids for injection into an ICP mass spectrometer has been described (9). In principle, this same concept should also be useful for nebulization of powdered solids that have been incorporated into a conducting pellet. This paper describes the results of our initial experiments to provide a technique for measurement of elemental or isotope ratios from pelleted powders without dissolution.

EXPERIMENTAL PROCEDURES

Pellet Preparation

Powdered samples were ground by hand to 200 mesh and mixed with graphite (Ultra Carbon, Ultra "F" purity grade UCP-1, 100 mesh) using a mechanical shaker. The mixture was poured into an aluminum sample cup and pressed hydraulically at a pressure of 4.8×10^7 Pa (7000 psi) into a disk-shaped pellet 2 cm diameter with a thickness of 3-5 mm. The relative proportion of sample to graphite was important in preparing the pellet. If too little sample was used, the detection limits suffered and distribution of the sample homogeneously throughout the pellet was difficult. A heterogeneous pellet yielded analyte count rates that were erratic because the arc wandered over heterogeneous surface layers during the nebulization cycle. Elemental analysis of nonconducting powders employed pellets that were 10-40% sample by weight. More concentrated pellets (up to at least 50% sample) could be used for conducting samples such as coal. Isotope ratio measurements for pure powders employed pellets that were 0.5-5% sample; more concentrated pellets tended to yield ions for the major constituents at too high a rate for linear response of the detector.

Instrumentation and Data Acquisition

The arc nebulizer has been described with other sources for optical spectroscopic measurements (10,11). The ICP-MS device (12) was

different from the common commercial versions in that no photon baffle was used in the ion lens. The background was thus higher but the sensitivity (i.e., slope of calibration curve) was comparable to or better than that obtained with the commercial device. A graphite pellet could be arced as long and as often as desired without noticeable plugging of the sampling orifice. Operating conditions were similar to those used during nebulization of metals (9) except that a slightly higher aerosol gas flow rate (0.7 L min^{-1}) was employed. The arc current was 3 amps. Material was eroded from the graphite pellet at a rate of approximately 0.5 mg min^{-1}, which was roughly half the erosion rate for a steel sample. This difference was probably due to the greater electrical resistance of the pellet (20-25Ω) relative to metal samples (~ 0.04Ω). The ion optical settings were adjusted to optimize signal for background ions with sample in place on the arc chamber but the arc off. These same voltage settings were also found to be optimum for transmission of analyte ions as found in our previous experience with this nebulizer and ICP-MS instrument (9).

Data were acquired using the mass analyzer in a repetitive scanning mode over a continuous m/z range with averaging of the resulting spectra. The signal averager employed had 4096 memory channels over the m/z range selected; dwell time was 40 μs per channel and 128 scans were typically taken and averaged to yield a spectrum from each sample. Thus, the data shown below were acquired while each sample was nebulized for approximately 20 s. Fast data acquisition with numerous iterations was preferred because the aerosol production fluctuated with time (9). Isotope ratios were determined by integrating the areas of selected

peaks and subtracting the background, which was evaluated by integrating a similar number of memory channels spanning a m/z range lacking a peak. A m/z window 6-15 daltons wide was scanned for isotope ratio determinations. Elemental ratios were determined from relative peak heights after background subtraction in a similar manner. Precision was evaluated by successive arcings of the same pellet, the surface of which was cleaned by hand between arcings. Various gain values for the electron multiplier were used by adjusting the applied potential, so the count rates reported below for different experiments are not always consistent with one another. Generally, a moderate bias voltage of -2.2 kV was used for the multiplier to avoid counting losses and split peaks. The various isotopes studied were assumed to be present in their natural relative abundances.

Several standard reference materials (SRMs) from the U.S. National Bureau of Standards were used. The rare earth ore standards used were supplied by the Materials Preparation Center of the Ames Laboratory. These rare earth standards were also analyzed as aqueous solutions by using ultrasonic nebulization and desolvation (13,14) with another ICP-MS device (ELAN Model 250, Sciex). Operating conditions used were similar to those described previously for analysis of U (15). Samples were dissolved in a $HClO_4$ and H_3PO_4 mixture in deionized water. The Ce results from solution analysis using this solvent were consistently below the concentrations specified for the standards. Failure to dissolve the Ce fully was suspected (16,17). Fresh batches of standards were then dissolved by refluxing with a solution of concentrated HNO_3 and H_2SO_4 in 1:1 proportions for 30 min. Analysis of the resulting

solutions after dilution with deionized H_2O yielded Ce concentrations in good agreement with the specified values.

RESULTS AND DISCUSSION

Mass Spectra

The mass spectrum obtained during nebulization of a blank graphite pellet is shown in Figure 1. As expected, C^+ was a major peak from the pellet. The peaks at m/z = 14 (probably $^{14}N^+$ but also possibly CH_2^+) and at m/z = 28 (probably CO^+) were also much larger than observed with aqueous nebulization. The O_2^+ peak was smaller than during injection of aqueous or metal aerosols; perhaps the carbon from the pellet induced a reducing atmosphere in the plasma. Reduction of the background level of O_2^+ facilitated determination of S using its major isotope at m/z = 32. The insert in Figure 1 shows an expanded view of the spectrum from m/z = 45-85. Small peaks were observed at m/z = 52 (probably ArC^+), 56 (probably ArO^+), and 80 (Ar_2^+). In general the background spectrum was simpler than during introduction of aqueous aerosol in agreement with previous observations made during arc nebulization of metals (9) and laser ablation (5). The sampling cone used had a smooth inner surface, which probably also was a factor in attenuating cluster ions as recently described by Hutton et al. (18). Little or no metallic peaks were observed indicating that metal impurities in the graphite were below the detection limit. The $^{40}ArH^+$ peak was not extremely large so that H might be determinable as ArH^+ as has been demonstrated with gas chromatographic sample introduction (19).

Some mass spectra of analytes from nebulized graphite pellets are shown in Figures 2 and 3. Metal oxide ions were not detectable above

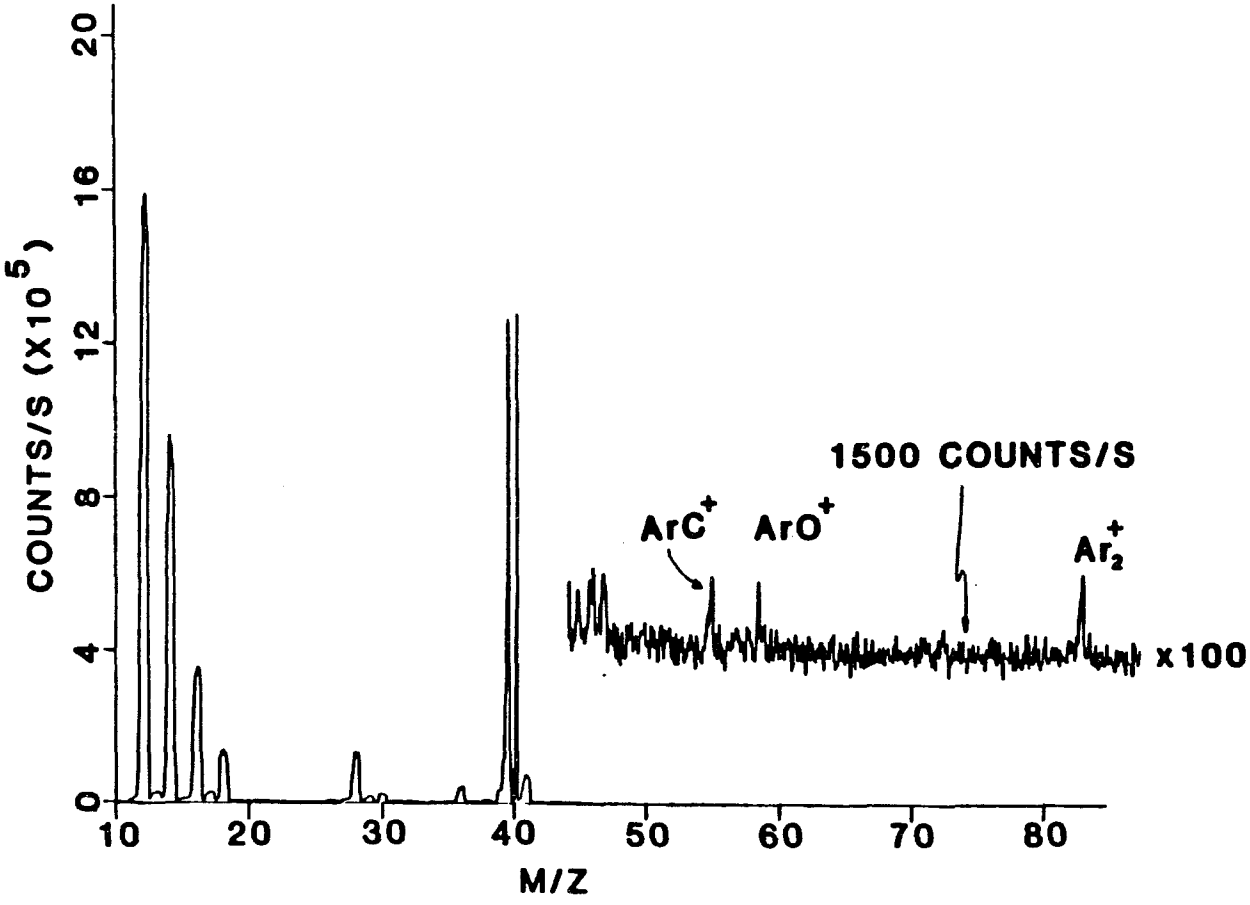

Figure 1. Mass spectrum obtained during nebulization of blank graphite pellet

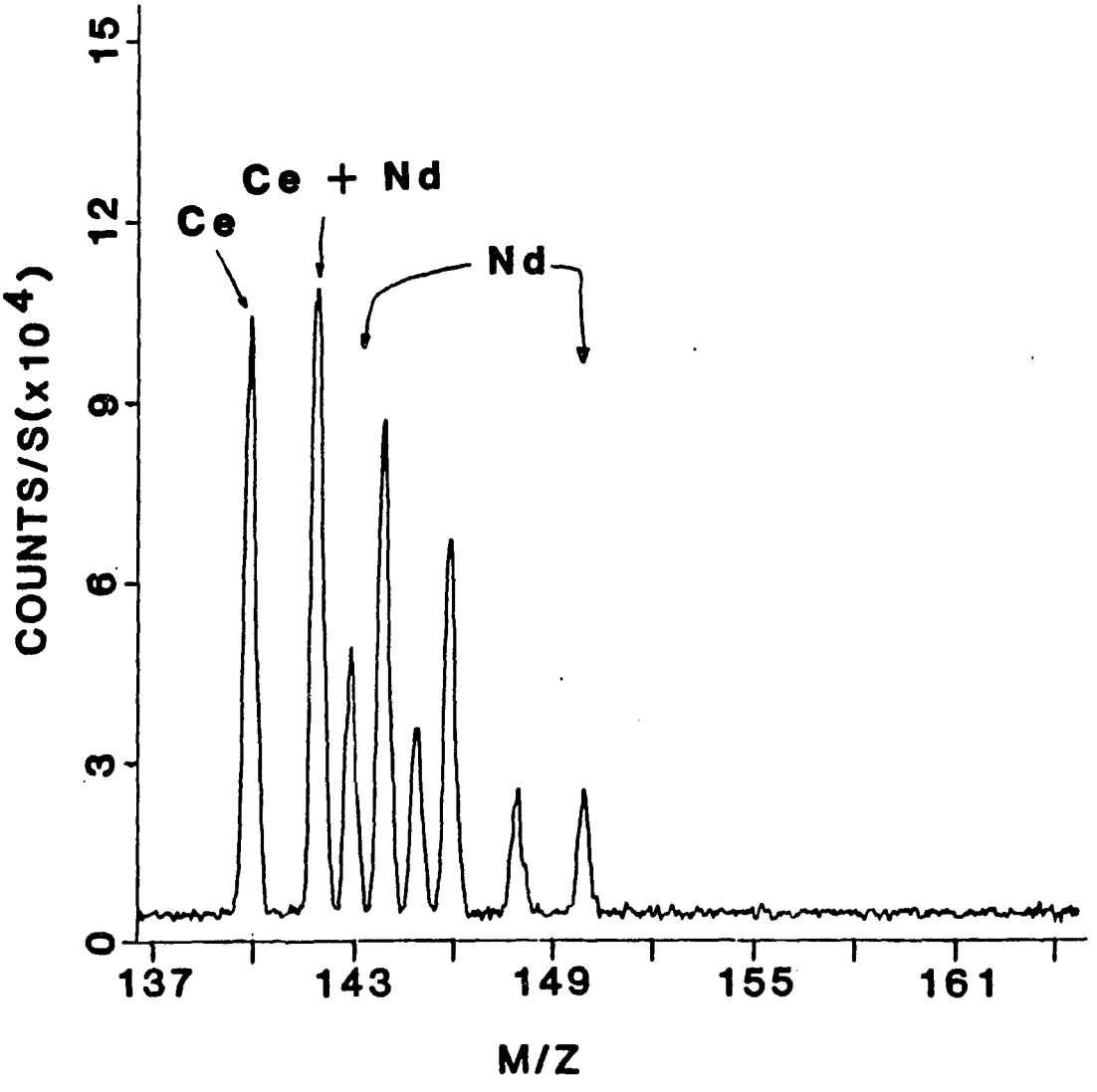

Figure 2. Mass spectrum of Ce (3.88%) and Nd (1.29%) as oxides in graphite pellet

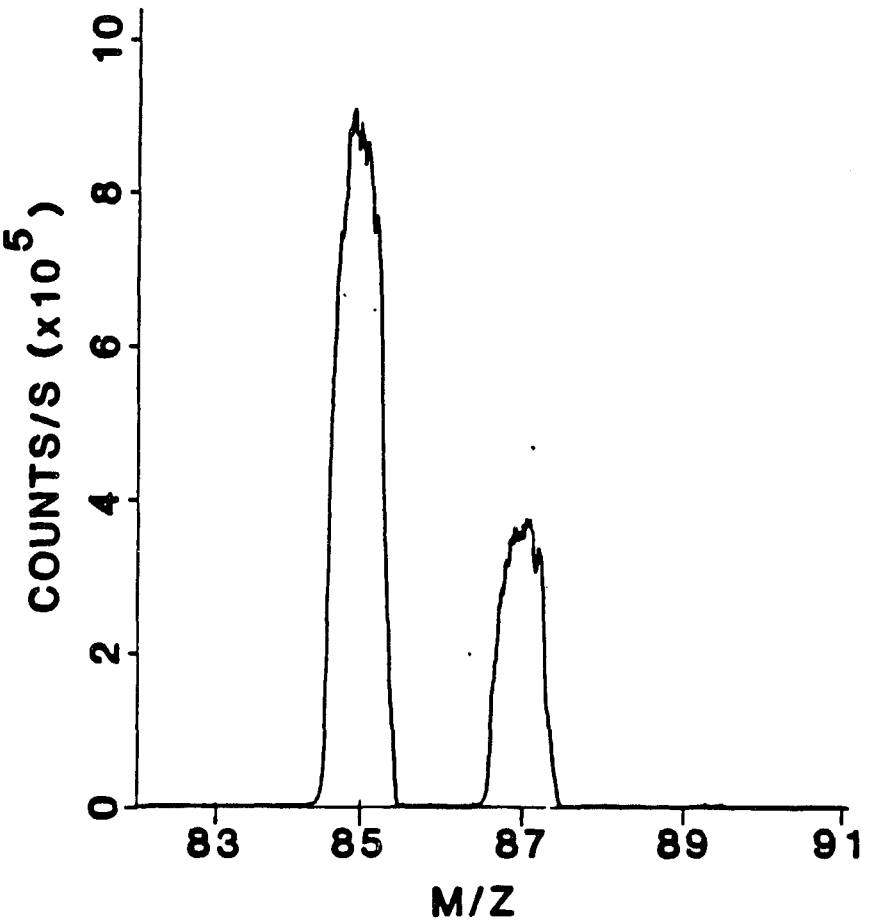

Figure 3. Mass spectrum of Rb as RbCl (4.01%) in graphite pellet

the noise in the background even for a pellet containing a high concentration of Ce (Figure 2), i.e., the ratio CeO^+/Ce^+ was 0.2% or less. This trend for dry sample introduction to suppress metal oxide ion formation (relative to oxide levels seen during aqueous nebulization) was again consistent with that observed from other solid sample introduction devices (5,9) and facilitated determination of heavy rare earths in the presence of the generally more abundant light rare earths. The levels of Ce^{+2} and Nd^{+2} observed during arc nebulization were approximately 2-3% of the M^+ ion. These levels of doubly charged ions were essentially the same as those during aqueous nebulization with ICP-MS device, for which a forward powder of 1.2-1.4 kW and aerosol gas flow rate of 0.6-0.8 L min^{-1} are typically used. The count rate for $^{85}Rb^+$ (Figure 3) was about the maximum desirable without counting losses. Formation of metal carbide ions was not observed ($MC^+/M^+ <$ 0.2%). The maximum ion kinetic energies observed in this work were $\leq$ 7 eV, i.e. considerably less than reported previously with the same ICP-MS instrument (20). The reasons for the lower ion energies may involve the dry sample introduction (21), but the grounding strap to the load coil has been replaced since ion energies were previously reported. Ion kinetic energies depend very critically on load coil geometry, grounding, shielding and ICP operating parameters for the type of coil used in the present work (20,21). Nevertheless, the results of lower ion energies are improved peak shapes and resolution than are apparent in previous spectra from this device.

The ability to identify elemental constituents in real samples was tested by arcing pellets containing powdered SRMs. A spectrum obtained

from a nonconducting sediment is shown in Figure 4. Elemental constituents at percent levels were easily observed and identified from the corresponding isotopic peaks. For example, the isotope ratios for S (m/z = 32, 33 and 34) were reasonably close to the expected natural ratios from the sediment sample. Other elements readily identified are Na, Mg, K, Fe and Cr. Manganese is easily detectable at 785 μg g^{-1} in the original sample. The insert shows that Zn, an element with a high ionization energy and unfavorable isotope distribution, is barely detectable at 1720 μg g^{-1}. Significant peaks for Ni (45.8 μg g^{-1}), Co (10.1) and Cu (109) were not seen, thus these elements are below the detection limits for this particular spectrum.

For Figure 4 the detector gain was deliberately kept at a medium value to prevent counting loss for species like Fe^+ and Na^+. Some improvement in detection limits could be obtained by increasing the voltage applied to the electron multiplier. A typical result is shown in Figure 5 for a pelleted coal. Mn was readily seen at 28 μg g^{-1}. The peaks at m/z = 51 and 52 were at least partially V^+ and Cr^+ at 44 and 34 μg g^{-1}, respectively. Perhaps zinc (m/z = 64 and 66) can be seen at 28 μg g^{-1}, whereas Cu and Ni at less than 20 μg g^{-1} cannot be discerned definitely from the background. The favorable dilution factor used to prepare this coal pellet and the conducting nature of the coal probably also contributed to these better detection limits relative to the sediment samples. These detection limits are poorer by factors of 10-20 than those obtained during arc nebulization of metals (9). A factor of 4 can be accounted for because the erosion rate for the graphite pellet is half that for metals and the sample comprises only half the pellet.

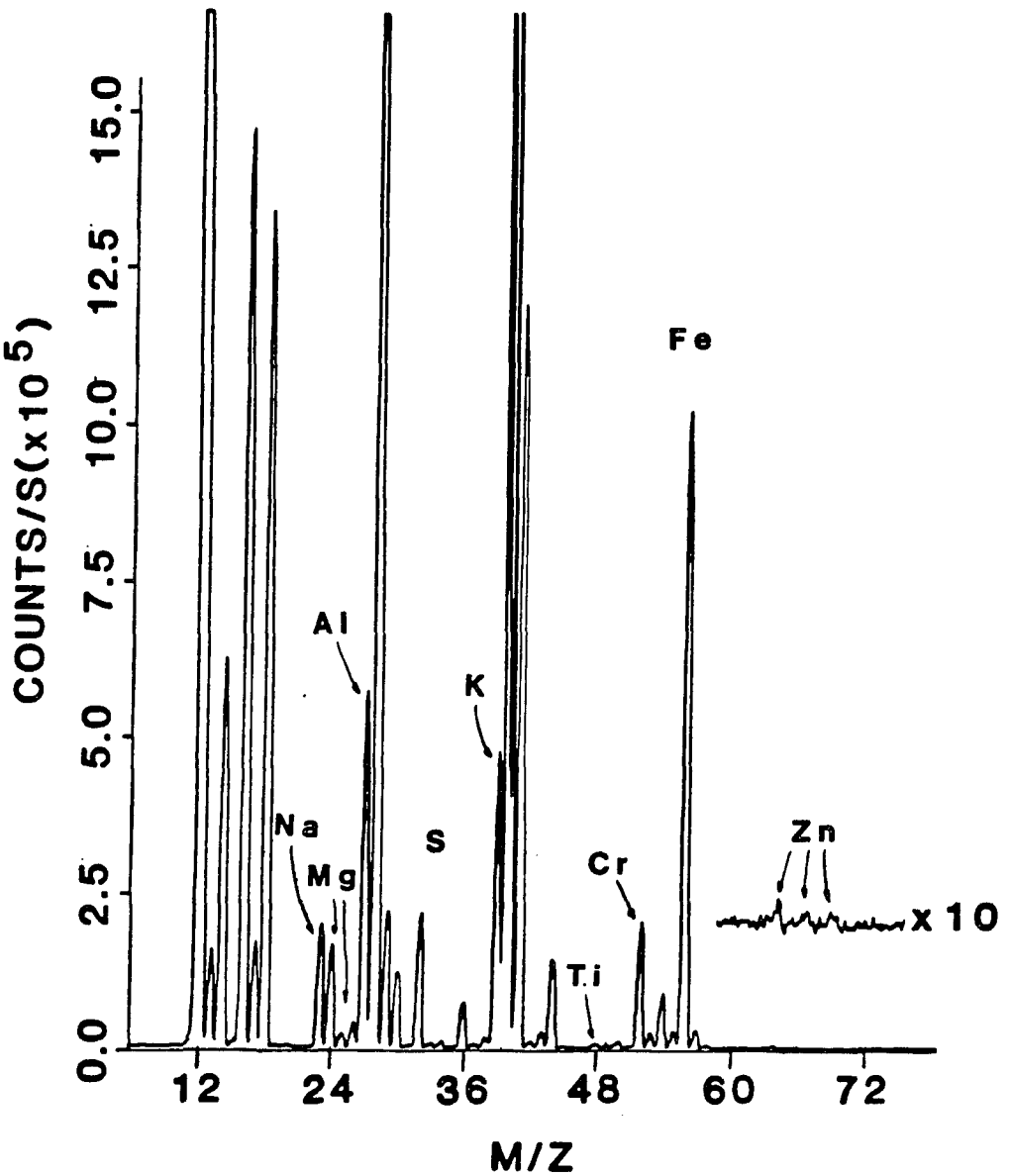

Figure 4. Mass spectrum from river sediment (NBS SRM 1645). Sample weight was 36% of total pellet. Minor constituents in weight % in the original sample are Na (0.54), Mg (0.74), Al (2.26), S (1.1), K (1.26), Cr (2.96) and Fe (11.3). Trace constituents in $\mu g\ g^{-1}$ are Mn (785), Ni (45.8), Co (10.1), Cu (109) and Zn (1720)

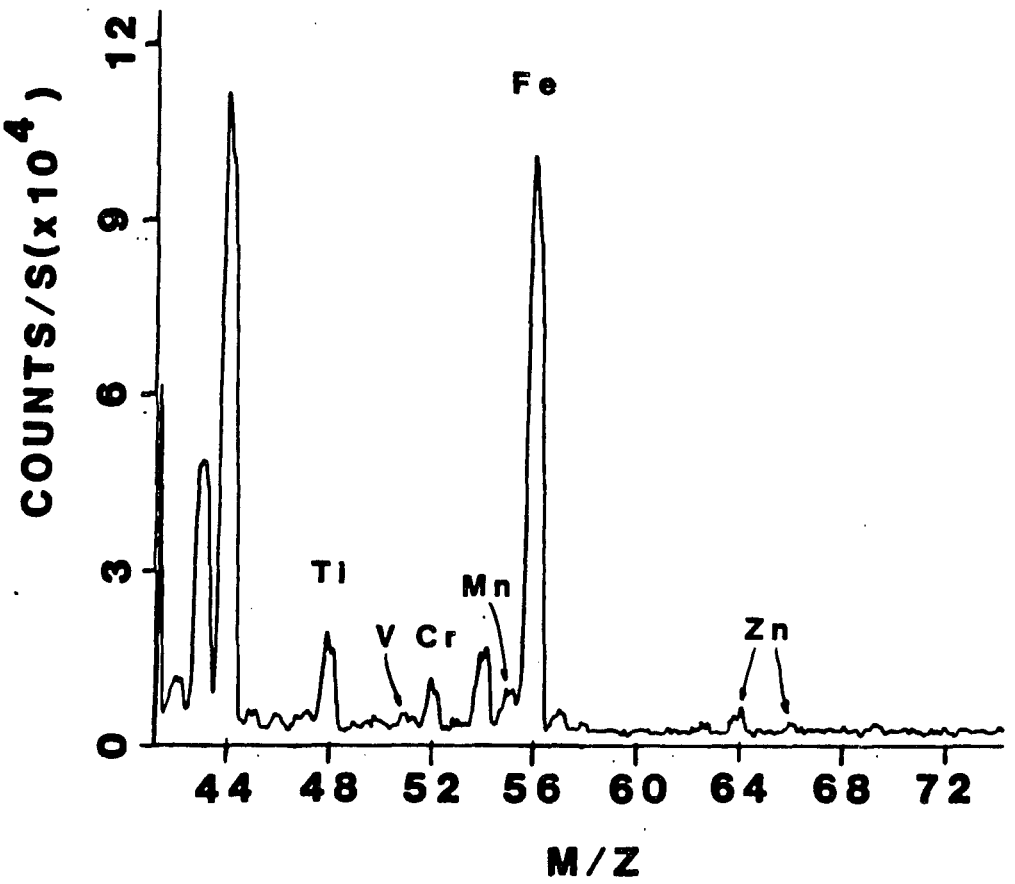

Figure 5. Mass spectrum from powdered coal (NBS SRM 1632) at 48% in pellet. Minor constituents in weight % in the original sample are Fe (1.1) and Ti (0.18). Trace constituents in μg g^{-1} are V (44), Cr (34.4), Mn (28), Ni (19.4), Co (6.8), Cu (16.5) and Zn (28). The detector was biased at -2.6 kV for this spectrum

The reason(s) for the additional differences in detection limits are unclear. Naturally, the detection limits could be improved (perhaps by a factor of 10) by selected ion monitoring and by further attenuating the background. Also, intense S^+ peaks were observed from the coal pellet with S at 1.58% in the original sample.

Isotope Ratio Determinations

Isotope ratio data for powdered pellets of various elements are listed in Table 1. One pellet was prepared for each element containing only the material listed and graphite. The precision for isotope ratios was generally 1% (relative standard deviation) or better for ratios close to unity. For these ratios the precision was comparable to that expected from counting statistics based upon the number of counts accumulated for each peak. As is usually the case with ICP-MS the precision tended to be poorer for naturally large or small ratios, and the experimentally-obtained precision also became worse than counting statistics by a factor of 2-7. However, the precision was still respectable (~ 5%) for the largest ratio determined ($^{164}Dy/^{160}Dy \simeq 12$). The accuracy in the determined ratios is also of the order of a few percent relative. The precision and accuracy from pelleted samples were similar to those obtained for the same instrument with other sample introduction techniques (e.g., gas chromatography) (19) and were comparable to or slightly poorer than when an ultrasonic nebulizer was used for continuous introduction of solution samples (12).

Table 1. Isotope ratio determinations by arc nebulization of pellets

Element (form)	Ratio	Determined	Natural	RSD (%)[a]
Ti (metal)	46/47	1.084	1.096	0.4
	46/48	0.111	0.108	1.7
	46/49	1.46	1.455	1.8
	46/50	1.509	1.539	2.2
Cu (metal)	63/65	2.154	2.236	0.8
Rb (chloride)	85/87	2.566	2.593[b]	1.4
Dy (oxide)	164/160	11.98	12.26	4.6
	164/161	1.489	1.492	2.4
	164/162	1.080	1.106	0.9
	164/163	1.114	1.133	1.9
Nd (oxide)	146/142	0.642	0.638	1.7
	146/143	1.356	1.430	0.2
	146/144	0.732	0.727	1.0
	146/145	1.985	2.084	0.7
	146/148	2.932	2.983	2.8
	146/150	3.038	3.089	3.2

[a]Relative standard deviation of 7 analyses of sample pellet.

[b]NBS SRM 984.

Quantitative Elemental Analysis of Mixtures

Rare earth elements were chosen because their behavior in ICP-MS has been extensively characterized (16,22) and because it was expected that their nebulization and ionization characteristics would be similar. A series of pellets was prepared with increasing concentrations of single rare earth oxides. Nebulization of these pellets yielded mass spectral peak heights that increased with concentration but the calibration curves showed unacceptable scatter and nonlinearity. Another series of pellets was prepared with increasing concentrations of one rare earth and a second rare earth added as internal reference. The resulting calibration curves were much improved with correlation coefficients of 0.9994-0.9999 (Figures 6 and 7). Thus, the internal reference compensated for individual variations in pellet properties. Correction of these curves for the different isotopic abundances and atomic weights of the elements yielded slopes close to unity, which showed that the nebulization efficiency and the response of the ICP-MS instrument were similar for the various rare earths.

Ratios of rare earths in several ore samples were determined. A typical mass spectrum is shown in Figure 8. Selection of a unique m/z value for each rare earth was straightforward because oxide ions were not a problem. In this particular spectrum sufficient Gd^+ was observed to permit its positive identification from the isotope ratios. Repeated nebulization of an individual ore pellet yielded isotope ratios for isolated peaks of Nd and Sm with a precision of approximately 2% (relative standard deviation) and accuracy similar to that indicated for

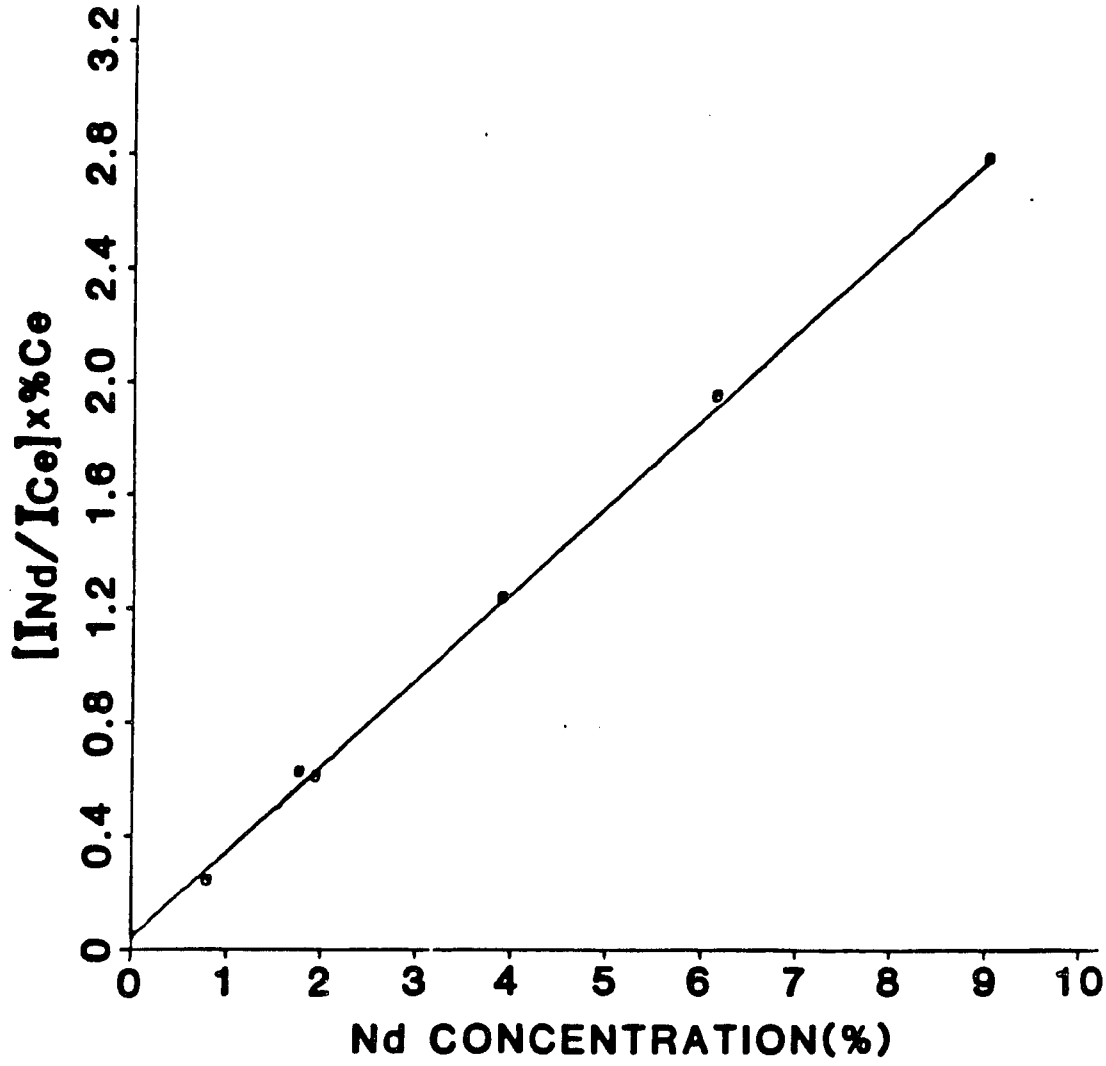

Figure 6. Calibration curve for Nd using Ce as internal standard. Correlation coefficient = 0.9994; net peak heights for ^{144}Nd and ^{140}Ce were used

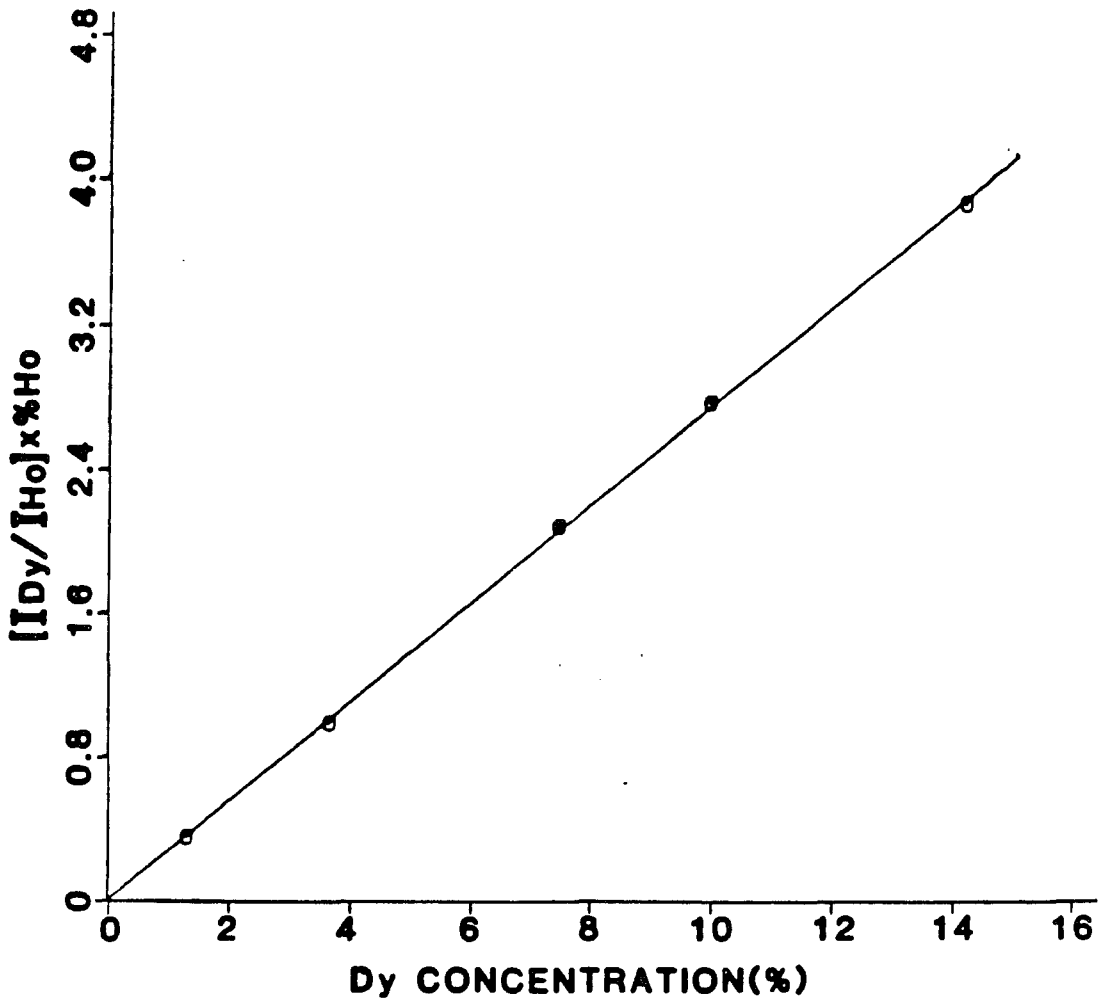

Figure 7. Calibration curve for Dy using Ho as internal standard. Correlation coefficient = 0.9999; net peak heights for ^{164}Dy and ^{165}Ho were used

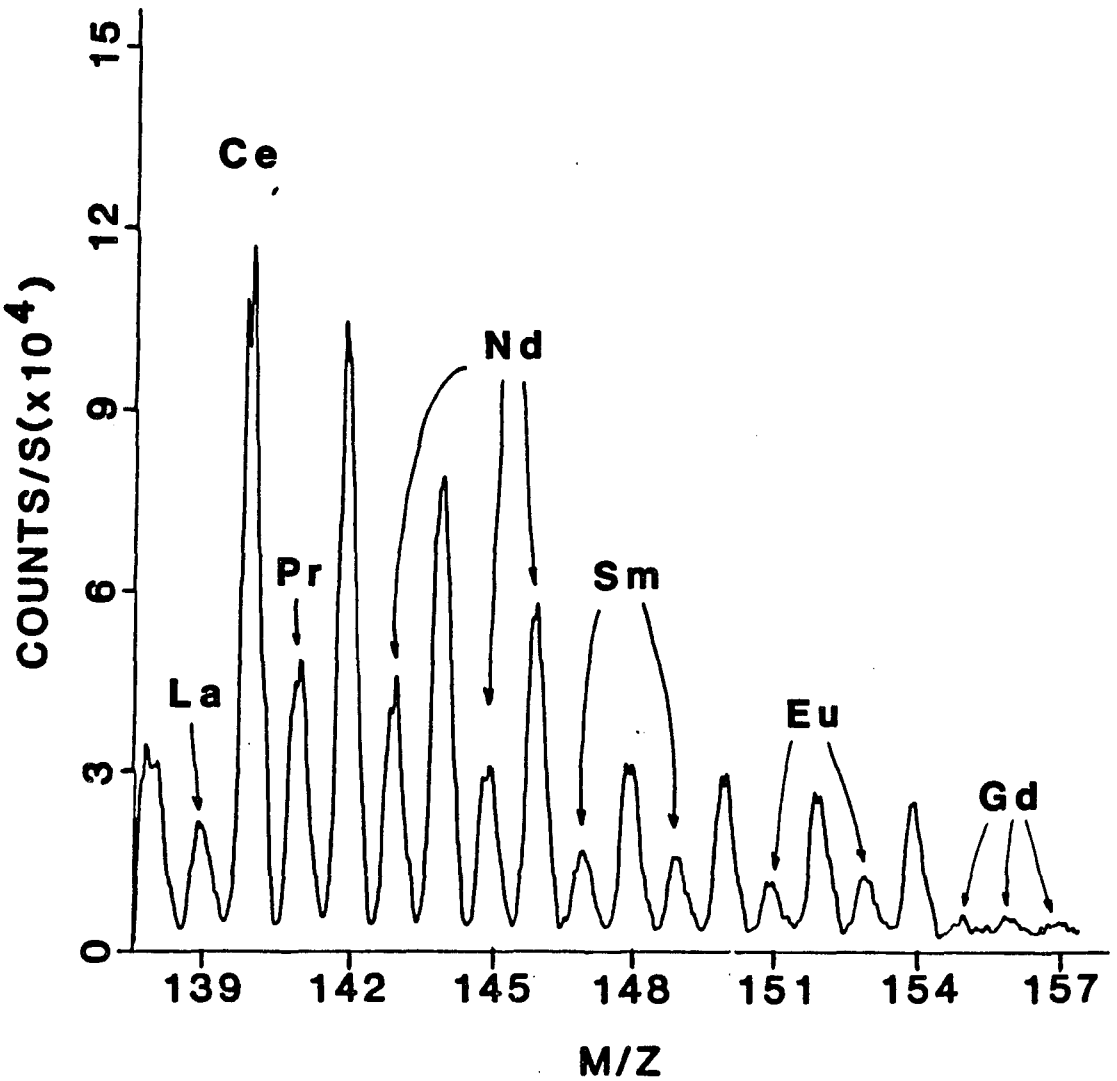

Figure 8. Mass spectrum of Lemki Pass ore (No. 58098) at 33.94% ore in graphite pellet

Table 2. Rare earth concentrations (in wt. %) determined for powdered Lemki Pass ore standards

		No. 58098		No. 59279	
Element	Isotope(s)	ICP-MS[a]	Other methods[b]	ICP-MS	Other methods
La	139	0.09	0.13, 0.09, 0.12	0.54	0.58, 0.42, 0.67
Ce	140	0.66	0.69, 0.76, 0.72	1.07	1.10, 1.12, 1.14
Pr	141	0.23	0.20, 0.26, 0.30	0.14	0.14, 0.05, 0.18
Nd	143	1.68[c]	1.68, 1.60, 1.77	0.65[c]	0.65, 0.45, 0.61
	145				
Sm	147	0.43	0.47, 0.23, 0.38	0.24	0.20, 0.12, 0.16
	149				
Eu	151	0.08	0.06, 0.03, 0.12	0.08	0.05, 0.03, 0.05
	153				
Gd	155	0.08	0.08, 0.08, 0.09	0.08	0.08, 0.08, 0.08

[a]Obtained by arc nebulization of powdered pellet with ICP-MS. Concentrations determined relative to ^{143}Nd assuming same instrumental response for different rare earths with correction for different atomic weights and isotopic abundances. The net peak height for the one or two most abundant isotopes free of overlap was used for each element.

[b]Values listed in the following order: (1) ICP-MS with solution nebulization and internal standardization with Lu, Ames Laboratory (15); (2) flame emission, Ames Laboratory (23) and (3) values supplied by Grand Junction Laboratory.

[c]The ^{143}Nd value determined by solution nebulization-ICP-MS was used as the reference value to convert the elemental ratios determined by arc nebulization-ICP-MS to actual concentrations.

Nd in Table 1.

Concentration values determined by arc nebulization-ICP-MS for two rare earth ore samples are compared with information values determined by other techniques in Table 2. Included in the "other techniques" was ICP-MS with aqueous nebulization (15). For the arc nebulization results the rare earths were determined relative to Nd. In general, the agreement between the values obtained by arc nebulization-ICP-MS was similar to the agreement among the information values. The arc nebulization results for Sm and Eu in standard No. 59279 were a bit higher than the information values provided. These results indicated that rapid qualitative and semiquantitative analyses of powdered solids can be performed by ICP-MS with arc nebulization without prior sample dissolution. Thus, this nebulization technique is a useful adjunct to ICP-MS for analysis of powders as well as metals.

LITERATURE CITED

1. Houk, R. S. Anal. Chem. 1986, 58, 97A.
2. Gray, A. L. Spectrochim. Acta, 1985, 40B, 1525.
3. Douglas, D. J.; Houk, R. S. Prog. Anal. Atomic Spectrosc. 1985, 8, 1.
4. Horlick, G.; Tan, S. H.; Vaughan, M. A.; Shao, Y.; Lam, J. 1986 Winter Conference on Plasma Spectrochemistry, Kona, HI, Paper No. 1.
5. Gray, A. L. Analyst, 1985, 110, 551.
6. Boorn, A. W.; Arrowsmith, P.; Gillson, G. 1986 Winter Conference on Plasma Spectrochemistry, Kona, HI, Paper No. 30.
7. Gray, A. L.; Date, A. R. Analyst, 1983, 108, 1033.
8. Boomer, D. W.; Powell, M.; Sing, R. L. A.; Salin, E. D. Anal. Chem. 1986, 58, 975.
9. Jiang, S.-J.; Houk, R. S. Anal. Chem. 1986, 58, 1739.
10. Jones, J. E.; Dahlquist, R. L.; Hoyt, R. E. Appl. Spectrosc. 1971, 25, 628.
11. Winge, R. K.; Fassel, V. A.; Kniseley, R. N. Appl. Spectrosc. 1971, 25, 636.
12. Olivares, J. A.; Houk, R. S. Anal. Chem. 1985, 57, 2674.
13. Olson, K. W.; Haas, W. J., Jr; Fassel, V. A. Anal. Chem. 1977, 49, 632.
14. Bear, B. R. M.S. Thesis, Iowa State University, Ames, IA, 1983.
15. Palmieri, M. D.; Fritz, J. S.; Thompson, J. J.; Houk, R. S. Anal. Chim. Acta, 1986, 184, 187.
16. Doherty, W.; Vander Voet, A. Can. J. Spectrosc. 1985, 30, 135.

18. Hutton, R. C.; Cantle, J. E.; Kelley, D. E. 1986 Pittsburgh Conference on Analytical Chemistry and Applied Spectroscopy, Atlantic City, NJ, Paper No. 229.

19. Chong, N. S.; Houk, R. S. Appl. Spectrosc. 1987, 41, 66.

20. Olivares, J. A.; Houk, R. S. Appl. Spectrosc. 1985, 39, 1070.

21. Gray, A. L.; Houk, R. S.; Williams, J. E. J. Anal. Atomic Spectrom. 1987, 2, 13.

22. Date, A. R.; Gray, A. L. Spectrochim. Acta, 1985, 40B, 115.

23. D'Silva, A. P.; Kniseley, R. N.; Fassel, V. A.; Curry, R. H.; Myers, R. B. Anal. Chem. 1964, 36, 532.

SECTION III.

CHROMATOGRAPHIC RETENTION OF Mo, Ti AND U COMPLEXES FOR REMOVAL OF SOME INTERFERENCES IN INDUCTIVELY COUPLED PLASMA MASS SPECTROMETRY

INTRODUCTION

Inductively coupled plasma mass spectrometry is a very sensitive technique for elemental and isotopic determinations (1,2). Most elements yield primarily singly charged, monatomic ions (M^+) so that analyte spectra are simple with limited overlap between peaks of different elements. The most abundant molecular species observed from analytes are the diatomic oxide ions MO^+, which cause overlap interferences with analytes 16-18 m/z units above M^+. Formation of metal oxide ions is a problem mainly for elements such as tungsten and the rare earths that form refractory oxide species in high temperature media. Such elements that are also multiisotopic generate the worst interference problems. Two particular interferences that have been noted are the overlap of MoO^+ with all the useful isotopes of cadmium (3), and overlap of TiO^+ with both copper isotopes and the most abundant zinc peak (4). Some elements also yield metal hydroxide ions (MOH^+), which further complicate matters (5-7).

At present, operating conditions can generally be identified for which the observed ratio MO^+/M^+ is 4% or less for elements that form the more stable oxide ions (1,2,8). As a rule of thumb, therefore, the error induced by oxide or hydroxide ion formation is significant only when the analyte is present at a concentration of a few percent or less relative to that of the interfering element. In many cases, the oxide contribution can be evaluated and subtracted from the total signal at the analyte m/z value to correct for the interference (6). Another conceivable approach is to find plasma operating conditions that

completely suppress MO^+. This measure may be realistic for "dry" sample introduction devices such as laser ablation (9) or arc nebulization (10). For introduction of aqueous aerosols, it is difficult to reduce the refractory metal oxide ions to less than 0.1% of the M^+ peak without having the plasma discharge strongly to the sampling orifice. A strong discharge generates ions from the orifice, yields excessive numbers of doubly charged ions, and causes high ion kinetic energies and other problems (5,11,12). It has recently been reported that use of a cooled spray chamber, aerosol desolvation, and/or a mixed Ar-N_2 plasma (13-15) helps reduce metal oxide levels somewhat. However, with the present performance of ICP-MS instrumentation, the analyst simply tolerates metal oxide ions. The resulting interferences usually are not severe, but they sometimes limit the accuracy achievable for some elements in certain types of samples.

An alternate approach to alleviating oxide interferences is to separate the interfering element(s) chemically or chromatographically so that they never reach the plasma. Use of chromatographic conditions that retain only the interferent and allow the analyte to flow freely through the column would accomplish this on a rapid time scale. The previous work of Al-Biaty and Fritz on the properties of the chelating reagent N-MFHA indicates that this compound is potentially useful for these separations. Conditions can be adjusted such that only ions with metals in highly positive oxidation states (usually +4 or higher) are complexed by N-MFHA. Under these conditions, ions with metals in lower oxidation states are complexed only to a slight extent or not at all. The metal complexes are readily retained by a short column containing

polystyrene divinylbenzene resin; the uncomplexed metal ions are not retained and wash rapidly through the column (16). Several metals that can cause significant oxide interference in ICP-MS also form stable complexes with N-MFHA at pH values that are sufficiently acidic that other potential analyte elements are not complexed. In the present work, titanium (IV) and molybdenum (VI) are selectively removed from analytical samples by complexation with N-MFHA and sorption on a resin column. Interference from TiO^+ and MoO^+ in the determination of copper, zinc, and cadmium by ICP-MS is thereby avoided.

Complexation of metals with N-MFHA is also potentially valuable for attenuating so-called "ionization interferences" in ICP-MS (15,17-21). Although virtually any element is capable of inducing such an interference, uranium can be one of the worst interferents (18,19,21). Furthermore, uranium oxide tends to deposit on the sampling cone and plug the sampling orifice to a greater extent than many other elements. If these deleterious effects could be circumvented, then ICP-MS would be very valuable for determination of trace impurities in uranium (21) because the mass spectrum of uranium is far simpler than its optical emission spectrum (22). The present work also shows that uranium (VI) can be readily complexed by N-MFHA and retained at a pH value that permits elution and determination of analyte elements such as rare earths.

EXPERIMENTAL

Apparatus

The ICP-MS device (ELAN Model 250, Sciex, INC.) has been described previously (21,23); for the present work, the upgraded ion optical system provided by Sciex was used. Operating conditions (Table 1) were optimized by the strategy described previously (21) and were generally similar to those used for other liquid chromatographic (LC) separations with ICP-MS detection (24).

The sample introduction system consisted of a dual piston pump (Model 2010, Varian), an injection valve and loop (50 µL unless stated otherwise), and a Hamilton PRP-1 column (150 mm long, 4.1 mm ID, 10 µm diam. particles). The outlet of the column (1.2 mL min^{-1}) flowed into a continuous flow ultrasonic nebulizer (26); the resulting aerosol was desolvated with a heating chamber at 200°C and a condenser at 0°C before being injected into the plasma. The dead volume after the column was approximately 13 µl in the liquid phase (24).

Reagents, Solvents, Standards and Samples

N-MFHA was prepared by the procedure outlined previously (16). The starting material was 2-furoyl chloride, which is a volatile irritant and should be handled with eye protection in a hood with adequate ventilation.

Solutions of molybdenum, titanium, cadmium, copper, and zinc were

Table 1. Experimental parameters

ICP torch	Ames Laboratory design (25) Outer tube extended to 40 mm from inner tubes
Ar gas flow rates:	
outer	14 L min^{-1}
auxiliary	0.8
aerosol	1.2
Forward power	1.25 kW
Sampling position	22 mm from load coil on center
m/z values monitored	
Ti	48
Cu	63
Zn	64 or 66
Mo	98
Cd	114
Tb	159
U	238
Data acquisition	Multiple ion monitoring (21) Three measurement positions per peak spaced 0.1 m/z unit about peak top Dwell time, 0.1 s at each measurement position Total measurement time, 1.5 s per peak

prepared by diluting aliquots of commercial stock solutions (Fisher Scientific). For isotope dilution experiments, isotopically enriched cadmium (as CdO, 96.53 atom % ^{116}Cd) and copper (as copper metal, 99.70 atom % ^{65}Cu) were obtained from Oak Ridge National Laboratory and dissolved in 1% HNO_3 in deionized distilled water. Aliquots of these stock solutions were mixed with the standard solutions in known amounts. Uranium was dissolved from $UO_2(NO_3)_2$ supplied by Fisher Scientific. Rare earth solutions were diluted from stock nitrate solutions supplied by Ames Laboratory.

Deionized distilled water with 2% methanol (HPLC grade, Fisher Scientific) and N-MFHA was used as the eluent for the titanium and molybdenum separations. The N-MFHA concentration was generally 0.003 M unless stated otherwise; in some experiments, a higher concentration of N-MFHA was necessary to keep the complexes in solution. The pH of the eluent was adjusted by adding concentrated HNO_3 and/or NH_4OH prior to the analysis. Molybdenum was separated from cadmium at pH = 1.0; titanium was separated from copper and zinc at pH = 2.2.

For uranium separations, the uranium (VI) complex with N-MFHA was retained at pH = 5.0. The eluent was 1% methanol in distilled deionized water with 0.001 M N-MFHA, 0.01 M pyridine, and sufficient HNO_3 to achieve the desired pH. Excess N-MFHA (2.4×10^{-3} M) was added to the samples before the injection. EDTA (1×10^{-4} M) was also added to the samples to mask rare earth analytes from the N-MFHA.

Several standard reference materials, for which oxide ion interferences had been noted in previous ICP-MS studies (3,4), were analyzed in the present work. These SRMs were the Ni base alloy BAS-346

(Bureau of Analyzed Samples, UK), and the marine sediments BCSS-1 and MESS-1 (National Research Council of Canada). The procedure used for dissolving the Ni base alloy employed redistilled, concentrated aqueous HNO_3 and HCl and has been described elsewhere (27). A similar procedure was used for the sediments. Naturally, the silica in these latter samples was not fully dissolved, so these digests were filtered and the filtrates were washed with 1 M HNO_3 several times.

After dissolution, the sample digests were diluted with deionized water so that the sample concentration was 0.4%. Quantification was done by standard additions to correct for any ionization interferences that may have occurred (4). The sample and three spiked samples were analyzed in each case. Calibration was performed using the net heights of the chromatographic peaks.

Determination of the titanium concentration in the sediment solutions indicated that only approximately 20% of the titanium was dissolved by the digested procedure (28). Analysis of these digests yielded good agreement between the certified and determined results for copper and zinc, but the concentration of interferent was artificially low (approximately 3 mg L^{-1} titanium). To provide a more rigorous test of the separation procedure, fresh samples were digested and analyzed after being spiked with a titanium stock solution to bring the total titanium concentration to approximately 27 mg L^{-1}. This level was 10 mg L^{-1} higher than what would have been obtained if all the titanium in the original sample had dissolved.

Measurement of Recovery

Solutions of copper, zinc and cadmium (250 mL, 1 mg L^{-1} each element) were complexed with N-MFHA (0.42 mM) at the desired pH. These solutions were passed through the column and the eluent collected. The collected eluents were then introduced continuously into the ICP (i.e., the column was bypassed), and the concentrations of copper, zinc and cadmium were determined by MS. The recovery was defined as the ratio of the count rate for the solution that had gone through the column to that for the original solution.

RESULTS AND DISCUSSION

Multiple Ion Chromatograms for Titanium and Molybdenum Separations

For the operating conditions used for the plasma and mass spectrometer, the ratios TiO^+/Ti^+ and MoO^+/Mo^+ were 0.2% and 0.5%, respectively. A multiple ion chromatogram obtained for a sediment sample spiked with additional titanium is shown in Figure 1. At the pH value indicated the titanium (shown at m/z =48) was efficiently retained by the column so that there was no overlap of TiO^+ isotope peaks with the copper and zinc peaks. For these chromatographic conditions, zinc eluted in the void volume slightly before copper. This difference was also apparent from Figure 2, which shows multiple ion chromatograms for two zinc isotopes and one copper isotope for several injections of sample and spiked samples of the MESS-1 sediment for the standard additions experiment.

As shown in Figure 3, cadmium at 0.1 mg L^{-1} was readily detected in the presence of a large excess of molybdenum (100 mg L^{-1}) because the N-MFHA complex of the latter was retained by the column. This separation was performed under more acidic conditions than the titanium - copper - zinc separation for reasons described below. The retention time for cadmium in Figure 3 was approximately the same as that for zinc in Figure 2, indicating that both elements eluted with the void volume. Injections of copper, zinc, and cadmium without N-MFHA present yielded the same peak heights as those shown in Figures 1 to 3, i.e., the presence of N-MFHA in the eluent did not affect the signal for Cu^+, Zn^+,

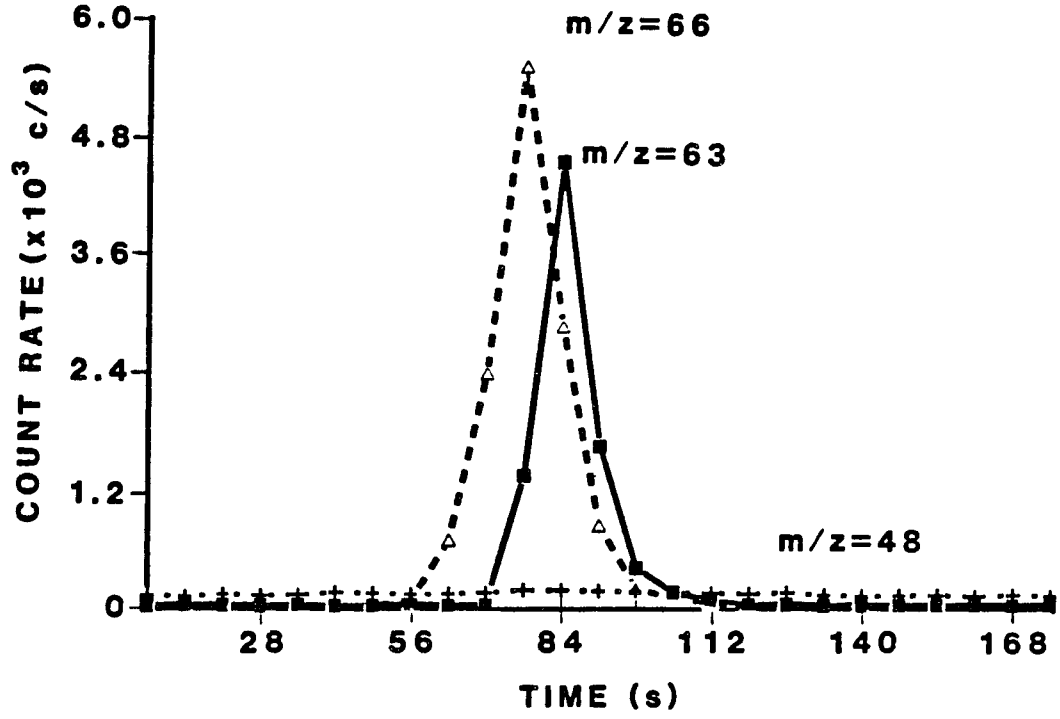

Figure 1. Multiple ion chromatogram for single injection of MESS-1 spiked with Ti at pH = 2.2. Concentrations in mg L^{-1} are Zn (0.76), Cu (0.10), Ti (27). (Δ) m/z = 66 (Zn); (■) m/z = 63; (+) m/z = 48 (Ti). The sample was injected at time = 0

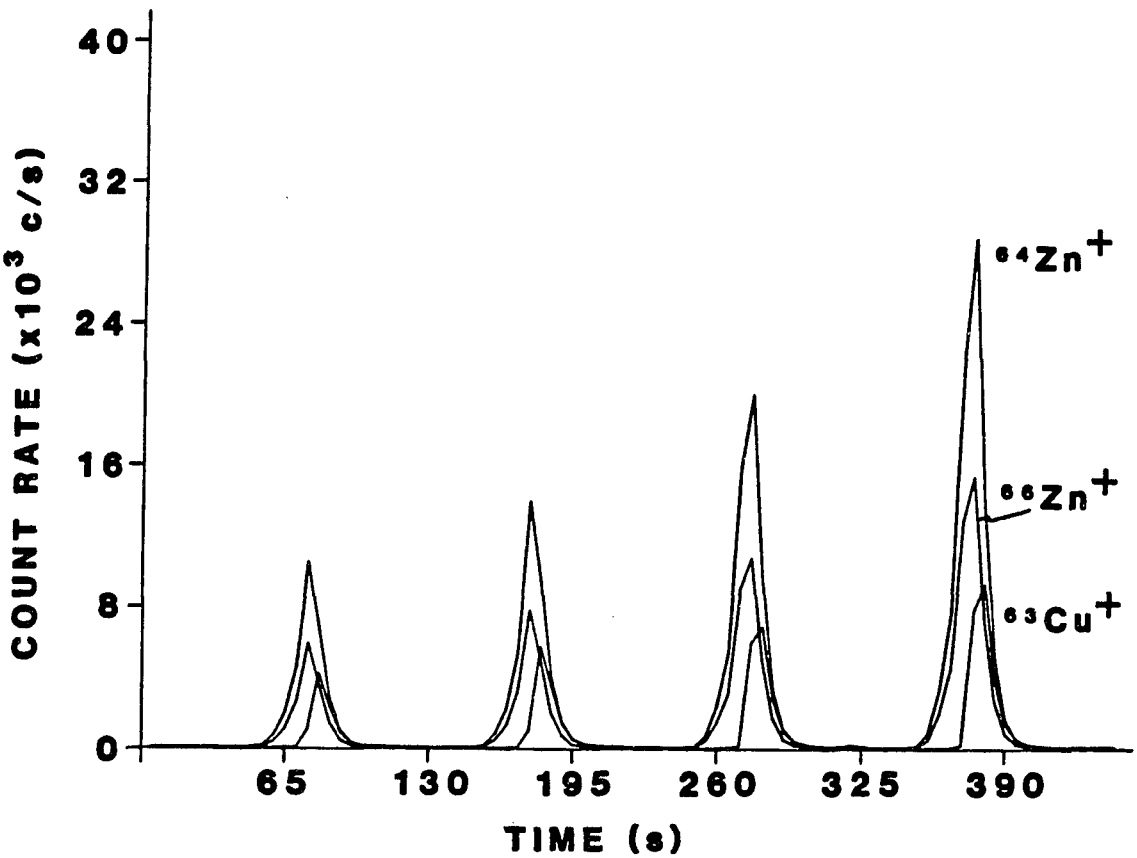

Figure 2. Multiple ion chromatogram for one injection of MESS-1 (left) followed by injections of three MESS-1 samples with spikes added for standard additions

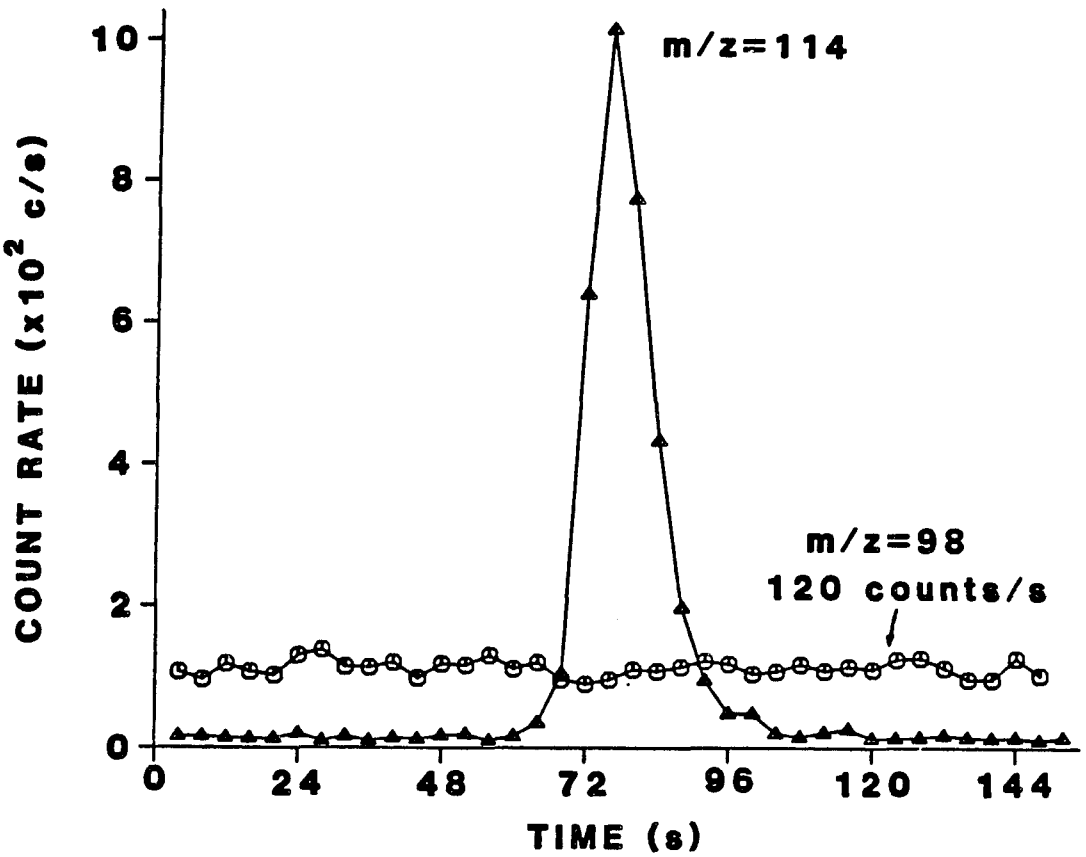

Figure 3. Multiple ion chromatogram for single injection of solution containing 0.1 mg L^{-1} Cd and 100 mg L^{-1} Mo. pH = 1.0. (Δ) m/z = 114 (Cd); (o) m/z = 98 (Mo)

or Cd^+. For these 50 μL injections, the chromatographic peak heights were approximately 30% of the steady state count rates, i.e., those obtained during continuous introduction of copper, zinc, or cadmium standards.

The slightly elevated count rates at m/z = 48 in Figure 1 and at m/z = 98 in Figure 3 were due mainly to small amounts of titanium and molybdenum eluting continuously from the column. This was verified by observing the correct isotope ratios for these elements when the appropriate m/z regions were scanned. In addition, a very small peak was eluted for titanium (approximately 30 counts s^{-1} net).

Analysis of Sediments and Nickel Base Alloy

Several standard reference materials were analyzed by the chromatographic ICP-MS procedure. The results are compared with the certified values in Table 2. The determined result for copper was slightly high and that for zinc was somewhat low for both sediments (MESS-1 and BCSS-1), but the deviations were within the uncertainties both for this particular measurement and those quoted by the suppliers of the reference materials. The cadmium in the final solution of the nickel base alloy (BAS-346) was only a factor of five above the detection limit (see below), yet the agreement with the certified value was reasonable. Except for the cadmium determination near the detection limit, the ranges cited in Table 2 were 2% to 4% relative to the mean. In each case, the standard additions curves were linear (correlation coefficient = 0.995 - 0.999).

Table 2. Elemental analysis of standard reference materials with separation of Ti and Mo complexes

Sample	Element	Analyte concentrations ($\mu g\ g^{-1}$) in original sample: Determined	Certified	Interferent concentration ($mg\ L^{-1}$) in final solution
BCSS-1 (sediment)	Cu	19.6 + 0.4 - 0.7[a]	18.5 ± 2.7[b]	27 Ti[c]
	Zn[d]	107 + 4 - 2	119 ± 12[b]	
MESS-1 (sediment)	Cu	26.8 + 0.5 - 0.7	25.1 ± 3.8[b]	27 Ti
	Zn[d]	183 + 4 - 2	191 ± 17[b]	
BAS-346 (Ni base alloy)	Zn[e]	30 ± 1	29 ± 2[f]	200 Ti
	Cd	0.48 ± 0.06	0.4 ± 0.05[f]	120 Mo

[a]Mean ± range of 3-4 analyses for all the determined values in this column.

[b]Uncertainties are 95% confidence limits.

[c]Titanium spike (approximately 24 $mg\ L^{-1}$) added to compensate for incomplete dissolution (see text).

[d]Zn monitored at m/z = 64.

[e]Zn monitored at m/z = 66 because of interference from $^{64}Ni^{+}$ and/or $^{32}S^{16}O_2^{+}$.

[f]Uncertainties are absolute standard deviations; the data supplied with the SRM use this measure of precision.

An additional "analysis" was performed by standard additions for a synthetic sample containing 500 mg L^{-1} titanium, 0.29 mg L^{-1} zinc, 300 mg L^{-1} molybdenum, and 0.020 mg L^{-1} cadmium. Five injections were made for each solution. The determined concentrations were 0.30 mg L^{-1} for zinc and 0.021 mg L^{-1} for cadmium, also in good agreement with the expected values. The agreement in this experiment and in the analysis of the reference materials (Table 2) indicated that the small leakage of titanium and molybdenum from the column did not yield significant TiO^+ or MoO^+.

Calibration curves were obtained for a series of cadmium standards (0.01 - 50 mg L^{-1}), each with 500 mg L^{-1} molybdenum. These calibration curves were linear (correlation coefficient 0.999 or better) up to the maximum cadmium concentration injected. Similar calibration curves were obtained for copper and zinc in the presence of titanium. For repetitive injections of solutions at concentrations similar to those for the peaks shown in Figures 1 to 3, the peak heights were reproducible to within a relative standard deviation of 3% - 7%, which is similar to the precision obtained in previous ICP-MS experiments with LC separations (24). These calibration curves were extrapolated to evaluate detection limits, which were the solution concentrations necessary to yield net peak heights equivalent to three times the standard deviation of the background at each m/z value of interest. The detection limits were 2 μg L^{-1} for copper, 1 μg L^{-1} for zinc, and 1 μg L^{-1} for cadmium at their most abundant isotopes. For zinc, the detection limit was a bit better than for copper because the background for copper at m/z = 63 was about 60 counts s^{-1} compared to 20 counts s^{-1}

for zinc at m/z = 64 or 66, and the standard deviation of the background was higher by a factor of approximately three at m/z = 63 as well. The detection limits were poorer by a factor of approximately 20 than what would be obtained for continuous nebulization of aqueous standards under similar operating conditions. The reasons for this degradation of detection limits when LC separations are used with ICP-MS detection include injection of a discrete sample, dilution by the eluent, and use of methanol in the eluent (24).

Isotope Ratio Determinations

Separation techniques are also of potential value for isotope ratio determinations, in which all the isotopes of interest should be free of overlap interference. Therefore, some isotope dilution experiments were performed for copper, zinc, and cadmium both with and without the potential interferent present. These results are shown in Table 3. In each case, the determined isotope ratios were the same whether titanium or molybdenum was present or not, which further indicated that oxide ion interferences were indeed negligible. The precision (1-2.5% RSD) was comparable to that achieved previously during multiple ion monitoring of individual chromatographic peaks (24) but was poorer than the 0.5-1% RSDs typically obtained for isotope ratio measurements for metals at mg L^{-1} levels during continuous introduction of aqueous solutions (23). Somewhat poorer precision in isotope ratio measurements is to be expected when transient sample introduction techniques are used because the ions of interest are observed for shorter times and averaging of

Table 3. Isotope ratio determinations with separation of Ti and Mo complexes

Elements injected (concentration, mg L^{-1})	Ratio	Isotope ratios		
		Determined[a]	RSD (%)	Expected[b]
Natural Cu (5)	$^{63}Cu/^{65}Cu$	2.28	2.0	2.24
Natural Cu (5) + Ti (200)	$^{63}Cu/^{65}Cu$	2.26	1.4	2.24
Natural Cu (5) + Enriched Cu (2) + Ti (200)	$^{63}Cu/^{65}Cu$	0.983	0.9	0.978
Natural Zn (5)	$^{64}Zn/^{66}Zn$	1.82	2.4	1.76
Natural Zn (5) + Ti (200)	$^{64}Zn/^{66}Zn$	1.82	2.6	1.76
Natural Cd (5)	$^{114}Cd/^{116}Cd$	3.68	1.7	3.79
Natural Cd (5) + Mo (200)	$^{114}Cd/^{116}Cd$	3.69	2.4	3.79
Natural Cd (5) + Enriched Cd (1) + Mo (200)	$^{114}Cd/^{116}Cd$	1.05	1.4	1.08

[a]Mean and relative standard deviation of 5 separate injections.

[b]Based on accepted natural abundances.

nebulizer fluctuations, etc., is less efficient. The slight but reproducible differences between the determined and expected values were comparable to those commonly seen in isotope ratio measurements with ICP-MS (23,29) and were probably caused by some mass discrimination in ion extraction, focusing, mass analysis, and/or detection. This experiment indicated that copper, zinc and cadmium could be readily quantified in the presence of excess titanium and molybdenum by isotope dilution (30) using the chromatographic ICP-MS procedure.

Column Capacities and Recoveries

Capacities for titanium and molybdenum complexes were determined by performing multiple injections of standards at 1000 mg L^{-1} and obtaining the resulting breakthrough curves (16) by monitoring Ti^+ or Mo^+ with the MS. The concentration of N-MFHA was 0.01 M. The measured capacity for molybdenum at pH = 1 was 200 µmole; for titanium at pH = 2.2, the capacity was 360 µmole. These values corresponded to approximately 400 injections of molybdenum and 360 of titanium for each element at 1000 mg L^{-1}. The actual mass of resin in this commercially obtained column was not known accurately but probably was about 0.5 g. After these capacity experiments, the resin was readily regenerated by rinsing with 1 M HNO_3 in methanol at a flow rate of 1 mL min^{-1} for approximately one hour.

Several injections were also made with very high concentrations of molybdenum or titanium. For these experiments, the concentration of N-MFHA was increased to 0.03 M to keep the complexes in solution. The resin retained nearly all (> 99%) of the metal complexes for single

injections of 11,300 mg L^{-1} molybdenum or 2000 mg L^{-1} titanium. However, the higher concentration of complexing agent in the mobile phase plugged the torch tip (not the sampling orifice of the mass spectrometer), so the ability of the resin to retain very large amounts of molybdenum or titanium was not of much practical value in the present study. The 1000 mg L^{-1} concentrations used in the capacity experiment represent a practical upper limit to the molybdenum and titanium levels that can be used with ICP-MS detection.

The recoveries for analyte elements were determined by the procedure described in the Experimental Section. For the molybdenum separation (pH = 1), the cadmium complex was 100% recovered. For the titanium separation (pH = 2.2), the recoveries were 104% for copper and 101% for zinc. The titanium complex was also retained efficiently at pH = 3, but recoveries for copper and zinc were only 92-93%, so separations at pH = 3 were not utilized further.

Alleviation of Interference from Uranium

A multiple ion chromatogram for several injections of terbium standards that also contained 100 mg L^{-1} uranium (as the complex in 1 mM N-MFHA) is shown in Figure 4. The U^+ signal would have been over 5 x 10^6 counts s^{-1} for each injection without the complexing agent present. However, the count rate at m/z = 238 was indistinguishable from the background (20 counts s^{-1}), which indicated that the uranium was retained very efficiently by the column. For the operating conditions chosen, the Tb^+ count rate would have been suppressed by 40% (relative

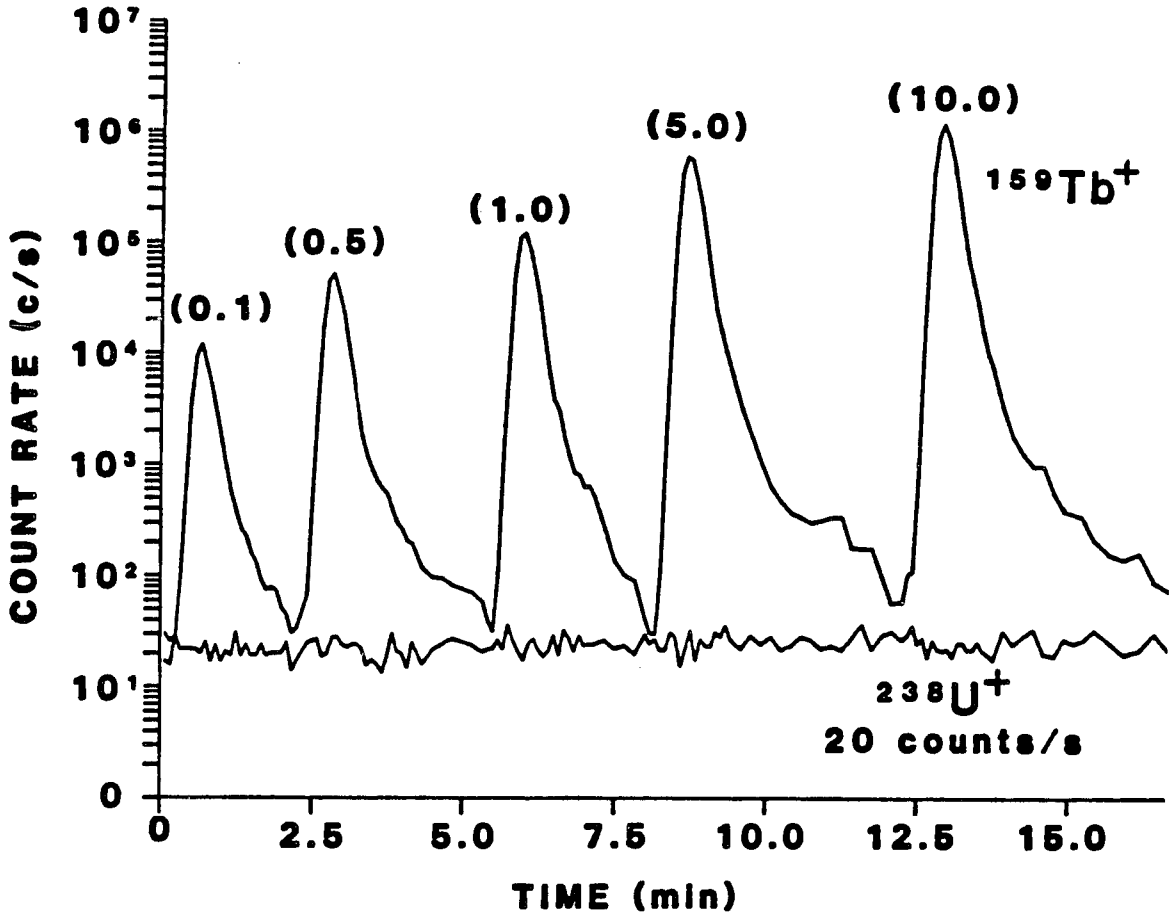

Figure 4. Multiple ion chromatogram for injections of various Tb standards (Tb concentrations given in mg L^{-1} in parentheses). Each standard also contained U at 100 mg L^{-1}. Note logarithmic scale on vertical axis

to the levels shown in Figure 4) if the standards had been injected without prior complexation and removal of the uranium. The terbium standards for Figure 4 also contained EDTA at 1×10^{-4} M; terbium recoveries were essentially quantitative with the EDTA present but were very low (< 10%) without EDTA. The peak heights shown in Figure 4 yielded a calibration curve that was linear with a correlation coefficient of 0.9998. For these 200 µL injections, the maximum Tb^+ signal reached approximately 60% of the steady level. For the latter two injections in Figure 4, the Tb^+ signal did not quite decay completely to the background in the four minute rinse interval employed. The rinse-out time requirement could be reduced by use of a fast flow cycle as shown by Fassel and Bear (26).

Similar results were obtained for the other rare earth elements, and many other potential analytes (e.g., thorium) are either not complexed by N-MFHA at pH = 5.0 (16) or would be masked by EDTA. This chromatographic separation should facilitate determination of a variety of elements in the presence of moderate amounts of uranium by ICP-MS (or ICP emission spectrometry, for that matter). The maximum solubility of the complex between N-MFHA and uranium (VI) corresponds to a uranium concentration of 470 mg L^{-1}, which limits the amount of uranium that can be present in the sample solution.

Other Possible Uses of N-MFHA

Complexation of interfering elements with N-MFHA may well be useful for avoiding other interferences encountered in ICP-MS. Iron (III) can

be efficiently retained at pH = 2.2. This capability could be used to prevent ionization interference (18) or oxide ion overlap (6) induced on analyte ions by excess Fe. Tin (IV) can also be efficiently retained at pH = 0.5. Tin has the most stable isotopes (ten) of any element. The combination of Sn^+ with any appreciable oxide or hydroxide ions would obscure most of the region m/z = 112 to 140 (or 141). These ions would interfere with one or more isotopes of Cd, In, Te, Cs, Ba, Ce and Pr. However, these analyte elements would be in oxidation states +3 or lower and should be easily separable from the tin (IV) complex with N-MFHA. Various other elements that form stable oxide ions (e.g., zirconium, hafnium, and tungsten) can also be separated from potential analyte elements as N-MFHA complexes (16).

Finally, the plasma operating conditions used were chosen by our normal process (21,23), in which minimizing oxide ions was an important criterion. These conditions generally yield rather less than the maximum M^+ count rates obtainable (4,21,23,31). With the Sciex ICP-MS device, the M^+ count rate can often be increased substantially by increasing the aerosol gas flow rate. These measures can also increase the abundance of oxide or hydroxide ions (4,31,32). If the oxide-forming elements can be removed chromatographically, plasma conditions that yield maximum M^+ signal and best detection limits could be used without severe interference from oxide ions of other elements. However, operation at relatively high aerosol gas flow rate also tends to yield worse ionization interferences (15,18) and poorer signal stability, the latter of which may require mass flow control of the aerosol gas flow rate.

LITERATURE CITED

1. Houk, R. S. Anal. Chem. 1985, 58, 97A.
2. Gray, A. L. Spectrochim. Acta, 1985, 40B, 1525.
3. McLeod, C. W.; Date, A. R.; Cheung, Y. Y. Spectrochim. Acta, 1986, 41B, 169.
4. McLaren, J. W.; Beauchemin, D.; Berman, S. S. J. Anal. Atomic Spectrom. 1987, 2, 277.
5. Houk, R. S.; Svec, H. J.; Fassel, V. A. Appl. Spectrosc. 1981, 35, 380; Dynamic Mass Spectrom. 1981, 6, 234.
6. Date, A. R.; Cheung, Y. Y.; Stuart, M. E. Spectrochim. Acta, 1987, 42B, 3.
7. Vaughan, M. A.; Horlick, G. Appl. Spectrosc. 1986, 40, 434.
8. Houk, R. S. "Plasma Ionization Techniques for Elemental Analysis by Mass Spectrometry, in Analytical Chemistry in the Exploration, Mining, and Processing of Materials", Butler, L. R. P., Ed.; Blackwell Scientific, Oxford UK, 1986, p. 25.
9. Gray, A. L. Analyst, 1985, 110, 551.
10. Jiang, S.-J.; Houk, R. S. Anal. Chem. 1986, 58, 1739.
11. Gray, A. L.; Houk, R. S.; Williams, J. G. J. Anal. Atomic Spectrom. 1987, 2, 13.
12. Douglas, D. J.; French, J. B. Spectrochim. Acta, 1986, 41B, 197.
13. Hutton, R. 1987 Winter Conference on Plasma and Laser Spectrochemistry, Lyon, France.
14. Horlick, G. 1987 Winter Conference on Plasma and Laser Spectrochemistry, Lyon, France.

15. Horlick, G.; Tan, S. H.; Vaughan, M. A.; Lam, J. 1987 Pittsburgh Conference and Exhibition on Analytical Chemistry and Applied Spectroscopy, Atlantic City, NJ, Paper No. 922.

16. Al-Biaty, I. A.; Fritz, J. S. Anal. Chim. Acta, 1983, 146, 191.

17. Olivares, J. A.; Houk, R. S. Anal. Chem. 1986, 58, 20.

18. Thompson, J. J.; Houk, R. S. Appl. Spectrosc. 1987, 41, 801.

19. Beauchemin, D.; McLaren, J. W.; Berman, S. S. Spectrochim. Acta, 1987, 42B, 467.

20. Gregoire, D. C. Appl. Spectrosc. 1987, 41, 897.

21. Palmieri, M. D.; Fritz, J. S.; Thompson, J. J.; Houk, R. S. Anal. Chim. Acta, 1986, 184, 187.

22. Winge, R. K.; Fassel, V. A.; Peterson, V. J.; Floyd, M. A. "Inductively Coupled Plasma-Atomic Emission Spectroscopy. An Atlas of Spectral Information", Elsevier, Amsterdam, 1985, Appendix A.

23. Serfass, R. E.; Thompson, J. J.; Houk, R. S. Anal. Chim. Acta, 1986, 188, 73.

24. Thompson, J. J.; Houk, R. S. Anal. Chem. 1986, 58, 2541.

25. Scott, R. H.; Fassel, V. A.; Kniseley, R. N.; Nixon, D. E. Anal. Chem. 1974, 46, 75.

26. Fassel, V. A.; Bear, B. R. Spectrochim. Acta, 1986, 41B, 1089.

27. Diehl, H.; Johnson, D. C.; Walters, R. R. "Laboratory Manual for the Course in Quantitative Analysis", Oakland Street Science Press, Ames, IA, 1985 ed., p. 15-2.

28. McLaren, J. W.; Berman, S. S.; Boyko, V. J.; Russell, D. S. Anal. Chem. 1981, 53, 1802.

29. Russ, G. P.; Bazan, J. M. Spectrochim. Acta, 1987, 42B, 49.

30. McLaren, J. W.; Beauchemin, D.; Berman, S. S. Anal. Chem. 1987, 59 610.

31. Horlick, G.; Tan, S. H.; Vaughan, M. A.; Rose, C. A. Spectrochim. Acta, 1985, 40B, 1555.

32. Vaughan, M. A.; Horlick, G. Appl. Spectrosc. 1986, 40, 434.

SECTION IV.

INDUCTIVELY COUPLED PLASMA MASS SPECTROMETRIC DETECTION FOR PHOSPHOROUS AND SULFUR COMPOUNDS SEPARATED BY LIQUID CHROMATOGRAPHY

INTRODUCTION

Since the development of ICP-MS in the late 1970s, this technique has been extensively developed for elemental and isotopic analysis. The analytical capabilities of ICP-MS, particularly the excellent powers of detection (generally 5 - 50 ng L^{-1}), also make it attractive as an element specific detection method for gas chromatography (GC) or liquid chromatography (LC) (1-4). The previous LC-ICP-MS reports have dealt only with detection of metals or metalloids. ICP-MS should also be of use for detection of some nonmetallic elements, primarily those for which the background peaks are not too high. In biochemistry, environmental chemistry, and many industrial applications, characterization of samples containing trace amounts of phosphorous and sulfur compounds (e.g., DNA, RNA, phospholipids, inorganic phosphates and sulfates, and various insecticides and fertilizers) is important.

Detection of phosphorous or sulfur in LC effluents by atomic emission spectrometry (AES) with excitation by an ICP or direct current plasma (DCP) has been studied by other investigators. Morita et al. showed the separation and quantitative determination of phosphate compounds using an LC-ICP-AES system (5). Heine et al. compared the UV and ICP-AES detectors for the determination of nucleotides (6). Yoshida et al. have determined twelve common 5′-ribonucleotides separately with the LC-ICP-AES system using a concentration gradient elution method (7). Biggs et al. determined polyphosphate distributions by LC with detection by DCP-AES (8). Yoshida et al. showed the separation and determination of amino acids with an LC-ICP-AES system by monitoring emission

intensities of carbon and sulfur (9). LaFreniere et al. have reported what are essentially the best results for LC-ICP-AES with their direct injection nebulizer (10). In this paper, we report results for ICP-MS detection of phosphorous and sulfur compounds separated by LC and compare these results to those obtained previously by AES detection.

EXPERIMENTAL

Chromatographic Apparatus and Conditions

The combined LC-ICP-MS device was similar to that described previously (3). A dual piston pump (Varian Model 2010) delivered solvent to either of two columns (Table 1). Each column was equilibrated with the ion pairing reagent and mobile phase prior to use. Samples were injected with a 50 µL loop injector (Rheodyne Model 7125). The column outlet was connected to the nebulizer of the ICP-MS device through stainless steel tubing (12 cm long, 0.25 mm ID), which had a dead volume of approximately 5 µL. All separations were performed at room temperature under isocratic conditions. Each separation was attempted under several different combinations of organic modifier concentration, type and concentration of counter ion, pH, etc. The conditions listed in Table 1 are those that yielded the best chromatographic resolution of the various sets tested.

ICP-MS Device and Conditions

These components are described in Table 2. The ICP-MS device was operated in a peak hopping mode (referred to as mulelm by Sciex) as described previously (3). Under these conditions, a data point could be obtained every second. The most abundant sulfur isotope (^{32}S) was not useful because of the major background ion O_2^+ at m/z = 32. The detection limits were estimated as the mass of element necessary to

Table 1. Separation conditions

Chromatographic parameters	Analytes: Inorganic phosphates	Adenosine phosphates	Inorganic sulfates	Amino acids
Column	Hamilton PRP-1 4 x 150 mm 10 µm	Hamilton PRP-1	Vydac 201 TP 4.6 x 250 mm 10 µm	Hamilton PRP-1
Ion pairing reagent[a]	$(TEA)NO_3$ 0.005 M	(TEA)Br 0.01 M	$(TBA)_3PO_4$ 0.005 M	(TEA)Br 0.01 M
Organic modifier	2% MeOH	5% MeOH	5% MeOH	1% ACN
pH	6	10	7.1	7.5
Flow rate of mobile phase	1.4 mL min^{-1}	1.6	1.4	1.2

[a]TEA = tetraethylammonium cation.

TBA = tetrabutylammonium cation.

Table 2. ICP-MS components and conditions

Nebulizer	Continuous flow ultrasonic nebulizer with aerosol desolvation Ames Laboratory construction (11) No mixing baffle in spray chamber Heating chamber 200°C Condensor 0°C
Nebulizer power supply	Model UNPS-1 Plasma Therm, Inc. (Now PF Plasma Products) Forward power 45 W Reflected power 10 W
ICP torch	Ames Laboratory construction (12) Outer tube 40 mm from inner tube
ICP conditions	Forward power 1.25 kW Reflected power 1 W Sampling position 25 mm from load coil On center Outer gas flow rate[a] 12 L min^{-1} Auxiliary gas flow rate 0.6 L min^{-1} Aerosol gas flow rate 1.2 L min^{-1}
ICP-MS device	ELAN Model 250 Sciex, Inc. (now Perkin Elmer-Sciex) with ion optics upgrade 1984
MS conditions	Ion lens voltages[b] B +5.4 V P -11.7 V E1, E3 -19.1 V S2 -5.4 V Dwell time 100 ms on each of 3 m/z positions spaced 0.1 m/z unit apart about peak top (3) Measurement time 0.3 s (3) m/z values 31 for P 34 for S

[a]All gas flows were comprised of argon.

[b]Refer to operating manual for identification of lens elements.

yield a net peak height equal to three times the standard deviation of the background at each m/z value of interest.

Reagents

Analytical reagent grade chemicals were used as supplied without further purification. The inorganic sulfates were obtained from Fisher, the inorganic phosphates were from Alfa Chemical Co., amino acids and nucleotides were from Sigma Chemical Co.

The mobile phases were prepared as follows. Ion pairing reagent PIC-A (tetrabutylammonium phosphate) was purchased from Waters Associates and dissolved at 0.005 M in HPLC grade organic solvent and deionized water. Tetraethylammonium bromide (Kodak) and tetrabutylammonium bromide (Alfa) were obtained in solid form. These were weighed and dissolved in organic solvent and deionized water to the desired concentration. HNO_3 (5%) and NH_4OH (1M) were added to adjust the pH to the desired value. The tetraethylammonium nitrate and tetrabutylammonium nitrate used in this study were prepared by titrating tetraethylammonium hydroxide (from Alfa as 40% aqueous solution) and tetrabutylammonium hydroxide (from Alfa as 55% aqueous solution) with redistilled HNO_3 in deionized water to the desired pH. Suitable amounts of organic solvents were added. The mobile phases were filtered through a 0.45 μm pore nylon filter and were degassed under light vacuum provided by an aspirator.

RESULTS AND DISCUSSION

Selection of ICP Operating Conditions

The performance of an ICP-MS device is strongly dependent on the operating conditions selected for the ICP (13,14). In the present work, the ICP conditions were selected to maximize the signal to noise ratio for P and S while continuously introducing a solution of 1 mg L^{-1} P (as KH_2PO_4) or 10 mg L^{-1} S (as Na_2SO_4) in the mobile phase to be used for the subsequent chromatographic separations. Compared to nebulization of aqueous solutions, a slightly lower aerosol gas flow rate and a slightly higher forward power were advisable because of the organic solvents present in the mobile phase; this is commonly observed for introduction of organic solvents into ICPs for either MS (15,16) or AES (17,18). The aerosol gas flow rate was adjusted first, then the forward power. The dependence of signal to noise ratio on forward power is depicted in Figure 1. This plot has the same general shape as the parameter behavior plots for introduction of aqueous aerosols reported by Horlick and co-workers (13,14). Although the background and background noise do change with forward power, the shape of the curve in Figure 1 is mainly determined by the trend of signal with power. In general, the same plasma conditions were also optimum, or nearly so, for S. The optimization process was repeated each day for each mobile phase used; the optimum conditions found differed slightly each time.

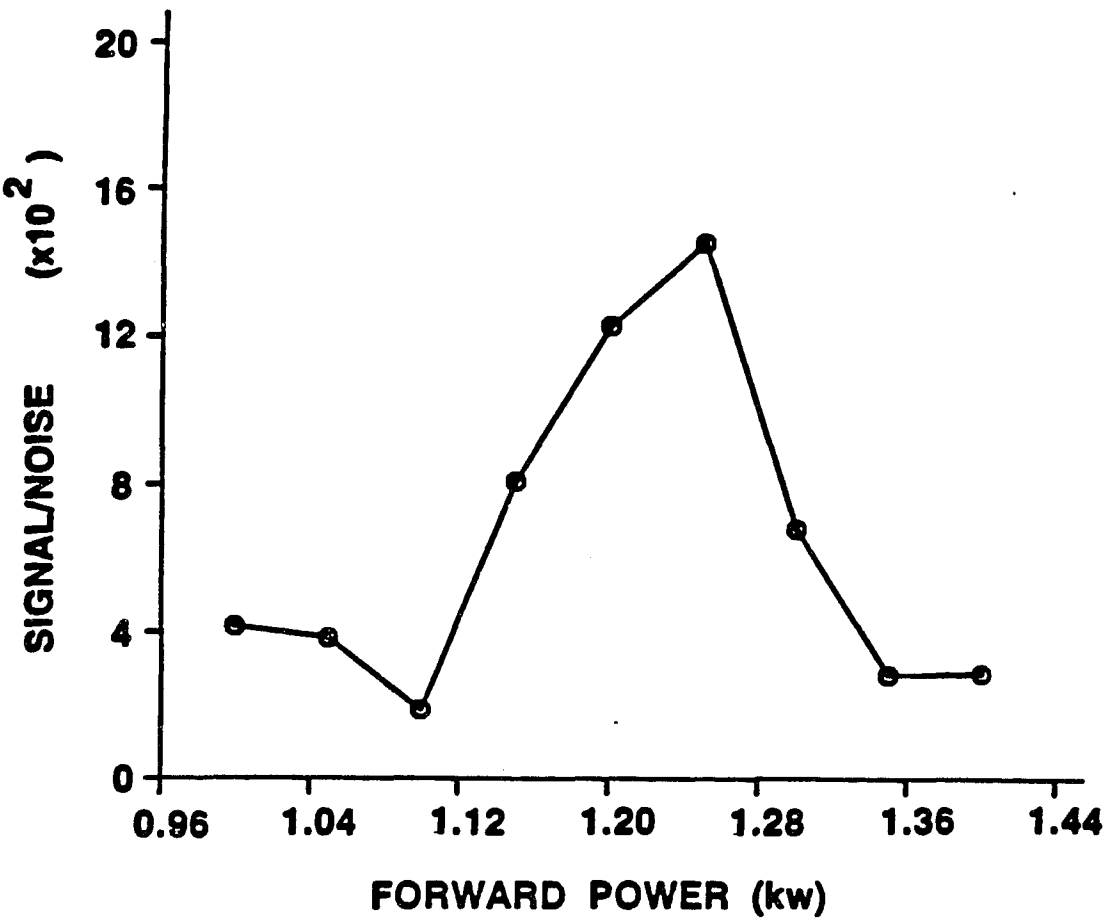

Figure 1. Dependence of signal to noise ratio for P (1 mg L^{-1} as KH_2PO_4) on forward power at aerosol gas flow rate = 1.2 L min^{-1}, mobile phase (5% methanol) flow rate = 2 mL min^{-1}

Inorganic Phosphates

A typical chromatogram of a solution containing PO_4^{-3}, $P_2O_7^{-4}$, and $P_3O_{10}^{-5}$, is shown in Figure 2. The pH was kept at 6 to avoid decomposition of $P_3O_{10}^{-5}$ reported at higher pH values (5). Peak area measurements indicated that the response for P was approximately equivalent (i.e., within ± 5% relative) for each of the three phosphates. Calibration curves based on peak heights were linear (correlation coefficient = 0.999) for each P compound in the range tested (20 µg P L^{-1} to 10 mg P L^{-1}). The detection limits were estimated from these calibration curves. The absolute detection limits were in the range 0.4 to 1 ng corresponding to relative values 8 - 20 µg P L^{-1} and are shown in Table 3. Although the background at m/z = 31 is high (~ 40,000 counts s^{-1}) compared to that seen for many other elements in ICP-MS, it is stable enough and P is ionized well enough for reasonable detection limits to be obtained. These detection limits are superior by factors of 200 to 2000 over the best LC-ICP-AES or LC-DCP-AES results reported for these inorganic phosphates.

Adenosine Phosphates

For these compounds, tetraethylammonium bromide was found to yield a better separation than the tetraethylammonium nitrate used for the separation of inorganic phosphates. A more basic mobile phase (pH = 10) was also necessary to insure that the adenosine phosphates were present as ions in the mobile phase. The PRP-1 resin-based column remained

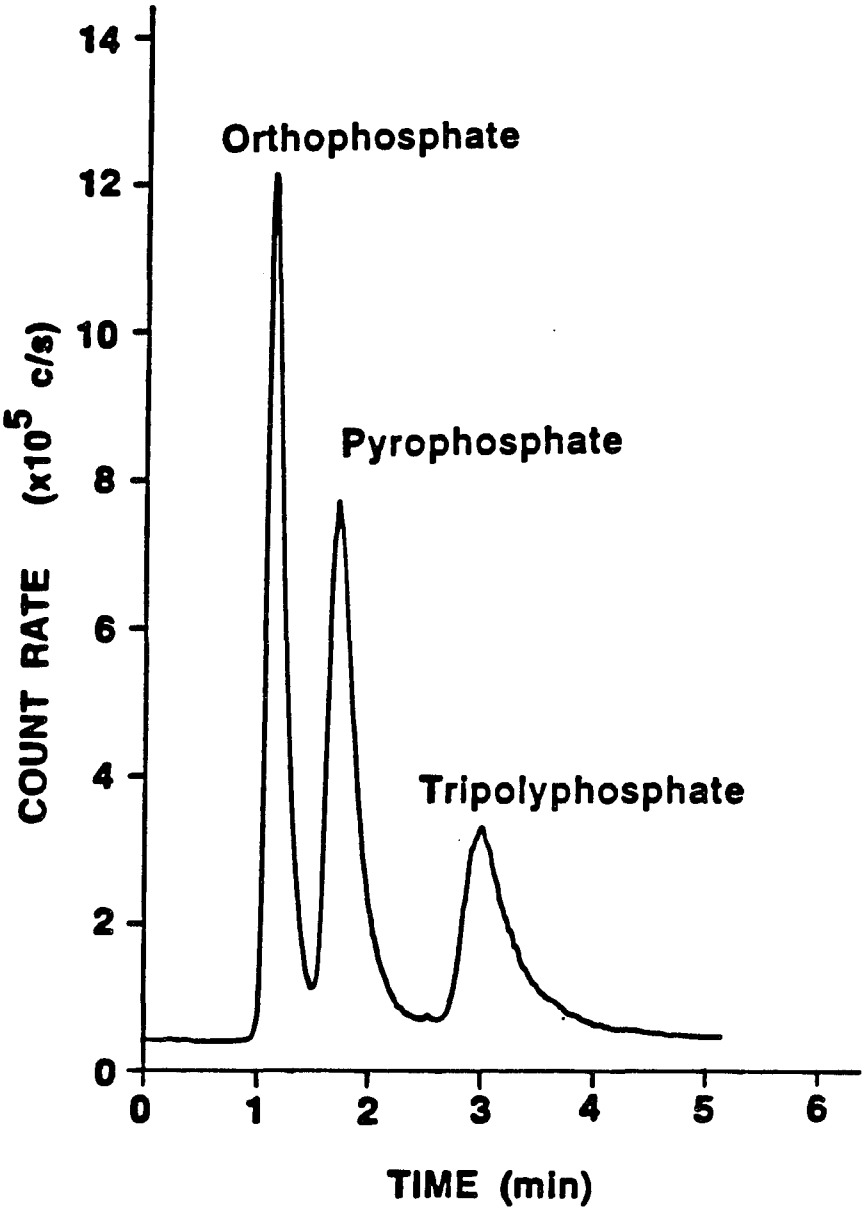

Figure 2. P-selective chromatogram showing separation of phosphates. Each form was present at 10 mg P L^{-1}. See Table 1 for chromatographic conditions for this and subsequent figures

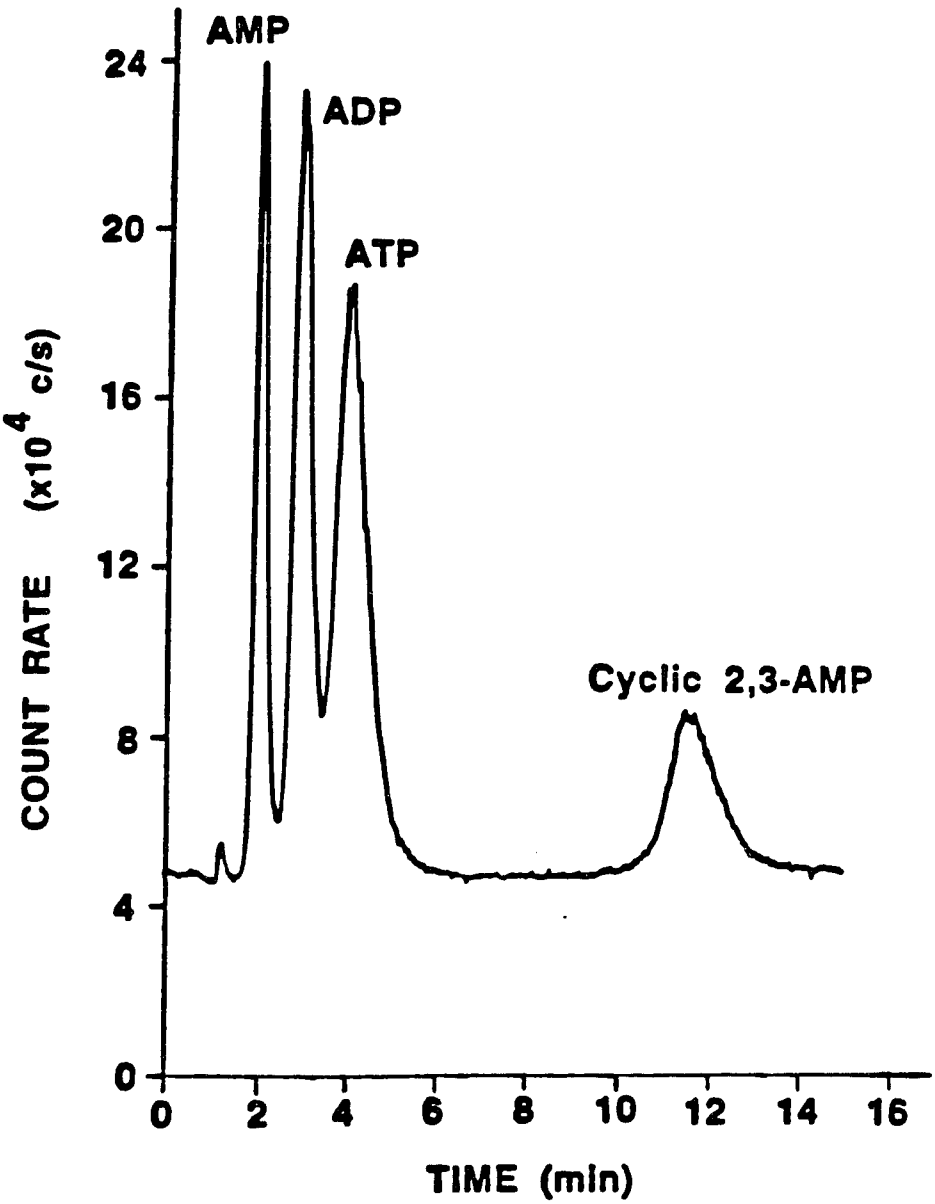

Figure 3. P-selective chromatogram for nucleotides, each present at following P concentrations: AMP (5 mg P L^{-1}), ADP (8 mg P L^{-1}), ATP (11 mg P L^{-1}), cyclic-2,3-AMP (5 mg P L^{-1})

Table 3. Phosphorous detection by ICP-MS

Compound	Detection limit (ng P) LC-ICP-MS (50 µL loop)	LC-ICP-AES or LC-DCP-AES
PO_4^{-3}	0.4	78[a], 160[b], 750[c], 500[d]
$P_2O_7^{-4}$	0.6	1000[d]
$P_3O_{10}^{-5}$	1	3000[d]
AMP	0.8	74[a], 750[c]
ADP	1.5	84[a]
ATP	2	92[a]
Cyclic 2,3-AMP	4	---

[a]Ref. (7), 200 µL Yoshida.

[b]Ref. (8), 20 µL Biggs.

[c]Ref. (6), 100 µL Heine.

[d]Ref. (5), Morita & Uehiro.

stable under these conditions, whereas a silica-based column would have been hydrolyzed.

A typical separation of four common adenosine phosphates is shown in Figure 3. The first small peak is from an impurity in the ADP because it was present when ADP alone was injected. The detection limits (Table 3) were in the range 0.4 to 4 ng P (absolute) or 16 to 80 μg P L^{-1} (relative) and were again superior to previous work with AES detection. The response of the ICP-MS device, as determined from the peak areas, was again similar for these four compounds. The response in Figure 3 differs from that in Figure 2 because the chromatographic conditions are different and the experiments were performed on different days, i.e., the sensitivity is not precisely reproducible from day to day.

Sulfates and Sulfur-Containing Amino Acids

A S specific chromatogram for sulfite and sulfate, and thiosulfate is shown in Figure 4. Sulfite and sulfate could not be separated under any conditions tested, perhaps because sulfite could have been converted to sulfate during the chromatographic process (10). Thus, the combined peak for sulfate and sulfite is twice as high as that for thiosulfate, indicating that the response factors for S were again independent of the compound, as was the case for P. The LC-ICP-MS detection limits were of the order of 150 μg S L^{-1} (Table 4). These detection limits were comparable or superior to the previous results obtained with AES detectors despite the low abundance (4.2%) of the ^{34}S isotope used in the present work.

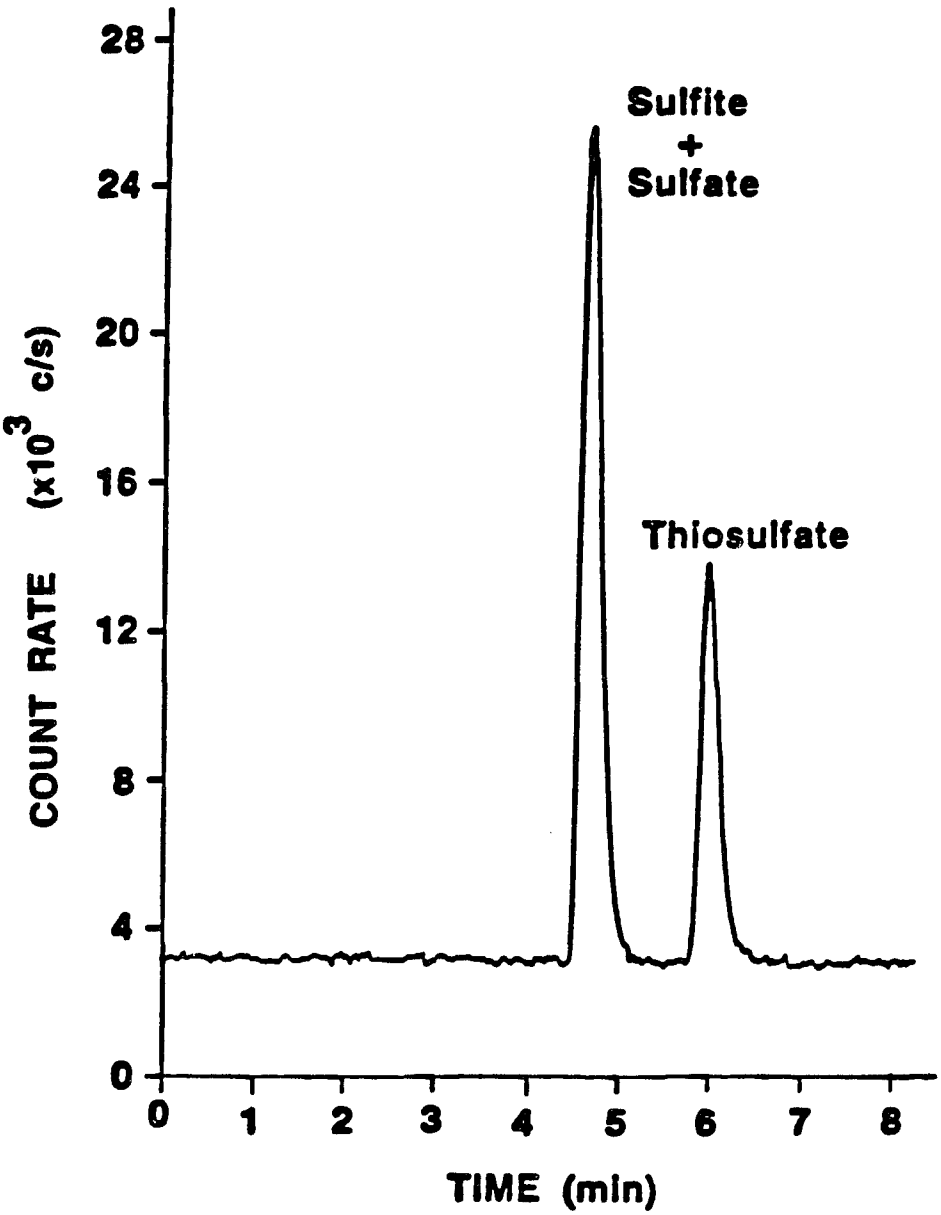

Figure 4. S-selective chromatogram for inorganic sulfur compounds, each present at 10 mg S L^{-1}, m/z = 34

Table 4. Sulfur detection by ICP-MS

Compound	Detection limit (ng S) LC-ICP-MS (50 µL)	LC-ICP-AES	LC-DIN-ICP-AES
SO_4^{-2}	7	---	16[b]
$S_2O_3^{-2}$	8	---	---
Cysteine & methionine	6	100-300[a]	

[a]Ref. (9), 100 µL Yoshida.

[b]Ref. (10), 100 µL LaFreniere.

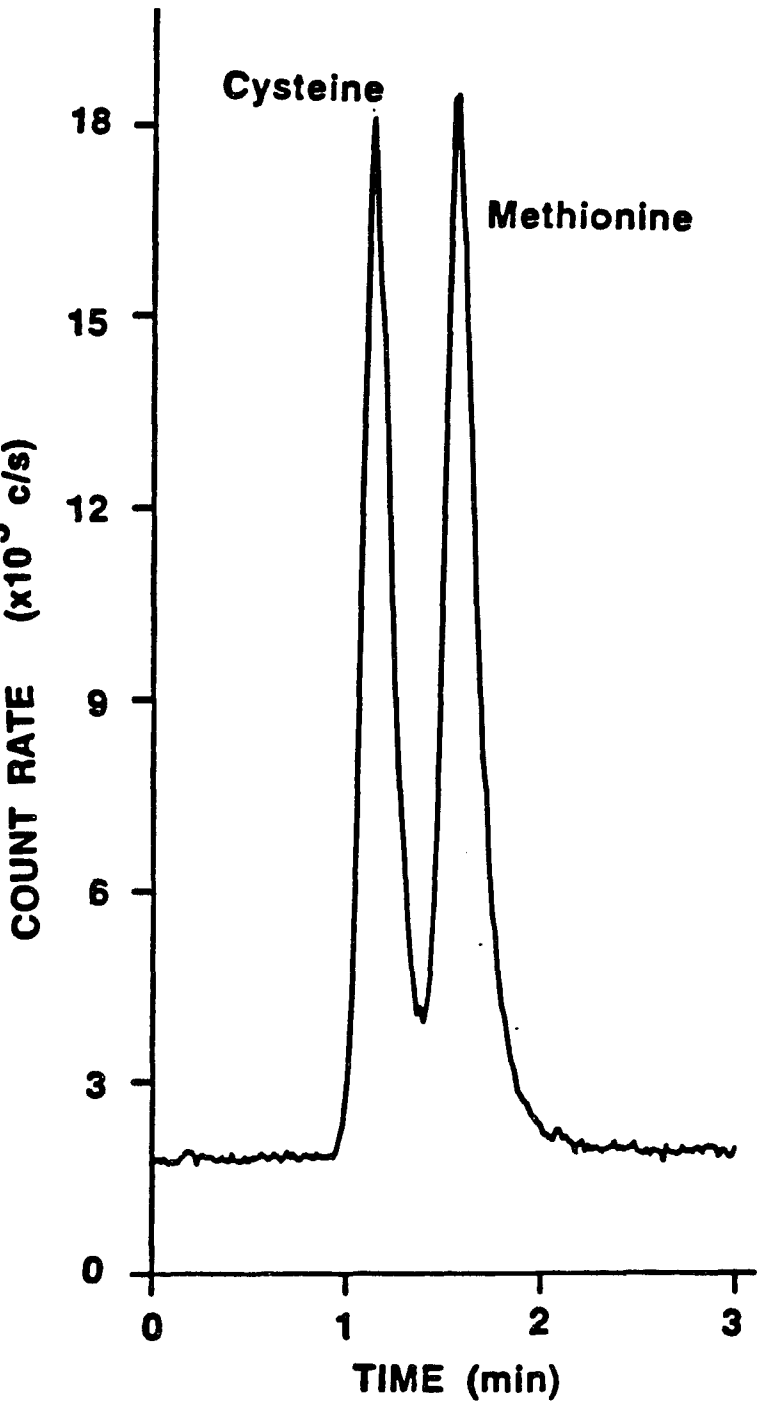

Figure 5. S-selective chromatogram for sulfur-containing amino acids, each present at 20 mg S L^{-1}

Finally, a S specific chromatogram for the amino acids cysteine and methionine is shown in Figure 5. Acetonitrile was used as the organic modifier in the separation. Detection limits were estimated to be 150 μg S L^{-1} in these compounds and were comparable to those found for the inorganic sulfates.

LITERATURE CITED

1. Chong, N. S.; Houk, R. S. Appl. Spectrosc. 1987, 41, 66.
2. Van Loon, J. C.; Alcock, L. R.; Pinchin, W. H.; French, J. B. Spectroscopy Letters, 1986, 19, 1125.
3. Thompson, J. J.; Houk, R. S. Anal. Chem. 1986, 58, 2541.
4. Jiang, S.-J.; Palmieri, M. D.; Fritz, J. S.; Houk, R. S. Anal. Chim. Acta, 1987, 200, 559.
5. Morita, M.; Uehiro, T. Anal. Chem. 1981, 53, 1997.
6. Heine, D. R.; Denton, M. B.; Schlabach, T. D. Anal. Chem. 1982, 54, 81.
7. Yoshida, K.; Haraguchi, H.; Fuwa, K. Anal. Chem. 1983, 55, 1009.
8. Biggs, W. R.; Gano, J. T.; Brown, R. T. Anal. Chem. 1984, 56, 2653.
9. Yoshida, K.; Hasegawa, T.; Haraguchi, H. Anal. Chem. 1983, 55, 2106.
10. LaFreniere, K. E.; Fassel, V. A.; Eckels, D. E. Anal. Chem. 1987, 59, 879.
11. Bear, B. R.; Fassel, V. A. Spectrochim. Acta, 1986, 41B, 1089.
12. Scott, R. H.; Fassel, V. A.; Kniseley, R. N.; Nixon, D. E. Anal. Chem. 1974, 46, 75.
13. Vaughan, M. A.; Horlick, G.; Tan, S. H. J. Anal. Atomic Spectrom. 1987, 2, 765.
14. Horlick, G.; Vaughan, M. A.; Rose, C. A. Spectrochim. Acta, 1985, 40B, 1555.
15. Hutton, R. C. J. Anal. Atomic Spectrom. 1986, 1, 259.
16. Hausler, D. Spectrochim. Acta, 1987, 42B, 63.
17. Blades, M. W.; Caughlin, B. L. Spectrochim. Acta, 1985, 40B, 579.

18. Nisamaneepong, W.; Hass, D. L.; Caruso, J. A. Spectrochim. Acta, 1985, 40B, 3.

SECTION V.

ALLEVIATION OF OVERLAP INTERFERENCES FOR DETERMINATION OF POTASSIUM ISOTOPE RATIOS BY INDUCTIVELY COUPLED PLASMA MASS SPECTROMETRY

INTRODUCTION

The development of ICP-MS has stimulated the study of mineral metabolism in humans by stable isotope labelling because the technique permits rapid measurements of isotope ratios for solution samples. Initial studies have verified that the accuracy, precision, and sensitivity are suitable for isotope ratio measurements for various elements (including Zn, Fe, Se, Cu, Pb and Li) in biological matrices such as feces, blood, and milk (1-6).

Potassium is an important element in various metabolic and physiological processes. Unfortunately, potassium does not have a good radioisotope for tracer studies (7). Stable isotopes of potassium could be used for either tracer experiments or for measurements of lean body mass (7) provided a rapid and convenient means for measuring the isotope ratios were available. The use of ICP-MS for these measurements has not been reported because the K^+ isotopes (m/z = 39, 40, and 41) are obscured by the intense background peaks from Ar^+ and ArH^+. One solution to this problem would be to use a plasma sustained in some gas other than Ar (8-13). Alternatively, this paper shows that Ar^+ and ArH^+ from an Ar ICP can be attenuated drastically simply by adjusting the plasma operating conditions. The sensitivity, precision, and effects of interferences are reported to evaluate the feasibility of this method for measurement of potassium isotope ratios.

EXPERIMENTAL SECTION

Instrumentation

A Sciex ICP-MS device (ELAN Model 250 with ion optics upgrade) was used. Operating parameters pertinent to this study are listed in Table 1. Note that two sets of parameters are listed. The "normal" set approximate conditions generally used for elemental analysis. These conditions yield typical background mass spectra including massive peaks at m/z = 40 and 41 (14,15). The parameters labelled "K isotopes" were used for the data reported in this study, in which these background peaks are attenuated.

The mass spectrometer conditions used for potassium isotope ratio measurements are listed in Table 2. The mass analyzer was operated by repetitive peak switching in an "isotopic scanning" mode. The total analysis time for each sample was approximately 120 s, in which the mass spectrometer measured ^{39}K for 36 s and ^{41}K for 72 s. Naturally, the reported isotope ratios were corrected for the different time spent on the two isotopes. The mean isotope ratios and relative standard deviations (RSD) were calculated from data for 7 repetitions of these 120 s measurements. Approximately 28 mL of solution were consumed for each set of seven determinations.

Samples were introduced with an ultrasonic nebulizer with desolvation of the resulting aerosol (17,18). Operating conditions for this device are listed in Reference (19), with the exceptions that the desolvation chamber was kept hotter than usual and uptake rate was 2 mL

Table 1. ICP-MS operating conditions

	Normal	K Isotope
Temperature of desolvation chamber	200°C	240°C
Forward power	1.25 kW	0.75 kW
Sampling position	25 mm from load coil	35 mm
Outer gas flow rate (Ar)	12 L min^{-1}	14 L min^{-1}
Auxiliary gas flow rate (Ar)	0.6 L min^{-1}	0
Aerosol gas flow rate (Ar)	1.2 L min^{-1}	1.6 L min^{-1}
Ion lens voltages		
B	+ 5.4 V	same
P	- 11.7	same
E1, E3	- 19.1	same
S2	- 5.4	- 1.8
Pressure in MS chamber	8 x 10^{-6} torr	1 x 10^{-5} torr

Table 2. Mass spectrometer conditions for isotope ratio measurements

Resolution[a]	low
Measurements per peak	3
Dwell time	100 ms
Measurement time	1.2 s
Repeats per integration	10
Cycle time	1 s

[a]Definitions and descriptions of these terms are given in the operating manuals and in refs. 2 and 16.

min^{-1} in the present work.

Solutions and Standards

Potassium and sodium solutions were prepared by diluting KCl or NaCl reference stock solutions (Fisher Scientific) with either deionized distilled water or 1% (v/v) HNO_3 in deionized distilled water. Doubly distilled concentrated HNO_3 was used to prepare the HNO_3 solutions. The isotope ratio $^{39}K/^{41}K$ in the standards was assumed to be the accepted natural value. This assumption was checked occasionally by analyzing a solution of potassium chloride standard reference material (No. 985, National Bureau of Standards) whose isotopic composition was certified. Within the uncertainties of the measurements, the determined ratio $^{39}K/^{41}K$ was essentially the same for either source of potassium, so the less expensive standard (from Fisher) was generally used. For the interference studies, a matrix blank containing sodium at its maximum concentration (100 mg L^{-1}) was also analyzed. This matrix blank did not contain measurable levels of potassium.

RESULTS AND DISCUSSION

Mass Spectra

The background mass spectrum obtained from the ICP under the "K isotope" conditions (Table 1) is shown in Figure 1. As indicated in Figure 1a, NO^+ (m/z = 30) was the major ion observed. Other background ions were O_2^+, O^+, H_2O^+, and H_3O^+. The three small peaks around m/z = 40 were a combination of residual Ar^+ and ArH^+ and some K^+, the latter of which probably came from potassium deposited on the sampler and/or skimmer. Despite this contamination, the background at m/z = 39 and 41 was only 50 counts s^{-1} or less. This spectrum was obtained after the sodium interference study, so a substantial Na^+ peak (m/z = 23) from deposited sodium was also seen. The plasma region sampled in this study was obviously cooler than for normal ICP sampling; consequently, the operating temperature of the sampler and skimmer were lower than normal. These components could be rebuilt to run hotter during operation, thereby minimizing deposition.

Compared to typical background spectra, the total ion signal shown in Figure 1 was far lower, and the common background ions were essentially replaced by NO^+. These observations were attributed to several general phenomena. First, the sampling position (35 mm from the load coil) was quite far from that corresponding to the top of the parameter behavior plot (~ 25 mm, Reference 19). Ion-electron recombination probably lowered the total ion density by the time extraction occurred. Second, entrainment of air both cooled the plasma

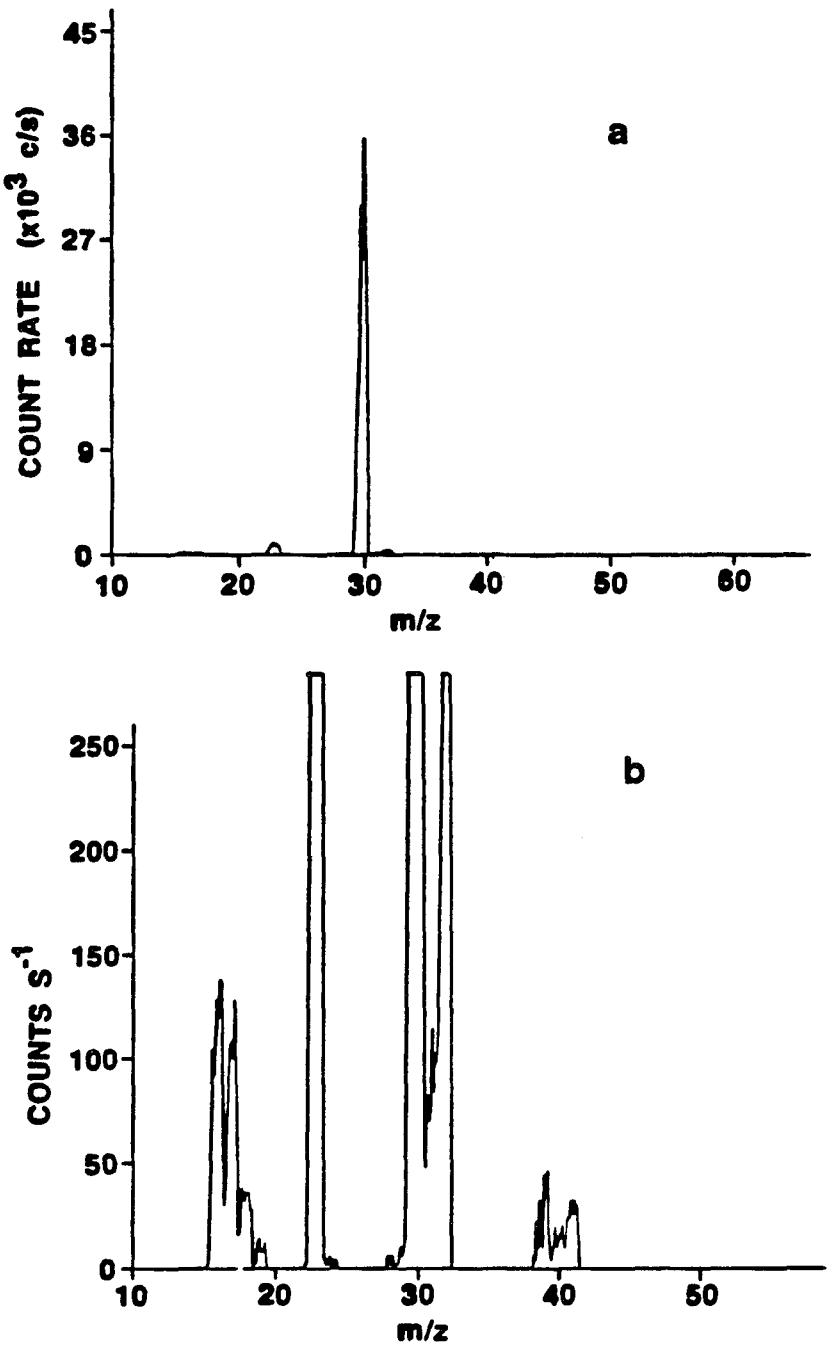

Figure 1. Background mass spectra obtained during nebulization of deionized distilled water. The same spectra are plotted with two different vertical scales

and added nitrogen and oxygen to it. A series of rapid ion-molecule reactions then converted the remaining ions to NO^+. Similar reactions also occur in certain regions of the earth's atmosphere and thus have been characterized extensively (20).

Douglas et al., in early ICP-MS studies, also observed that air entrainment into a "skimmed" Ar ICP could cause NO^+ to become the major background ion (21), and Gray reported similar observations caused by air impurities in a direct current capillary arc plasma (22). Both these groups noted that the sensitivity for elements with ionization energies greater than that of NO (9.27 eV) was limited, probably because such atomic ions would just be neutralized by exothermic charge transfer to NO. This effect is not a serious limitation in the present work because the ionization energy of K (4.34 eV) is much lower than that of NO.

A spectrum obtained during introduction of a potassium solution (10 mg L^{-1}) is shown in Figure 2. The two main potassium isotopes (m/z = 39 and 41) were clearly observed. A slight increase in the count rate at m/z = 40 was also observed due to the rare $^{40}K^+$ isotope, although this increase does not show up in Figure 2 because of the scale. The inclusion of potassium at only 10 mg L^{-1} induced a 75% loss of NO^+, and K^+ replaced NO^+ as the major component of the background spectrum. In both Figures 1 and 2, the background above m/z = 41 was very low (< 1 counts s^{-1}).

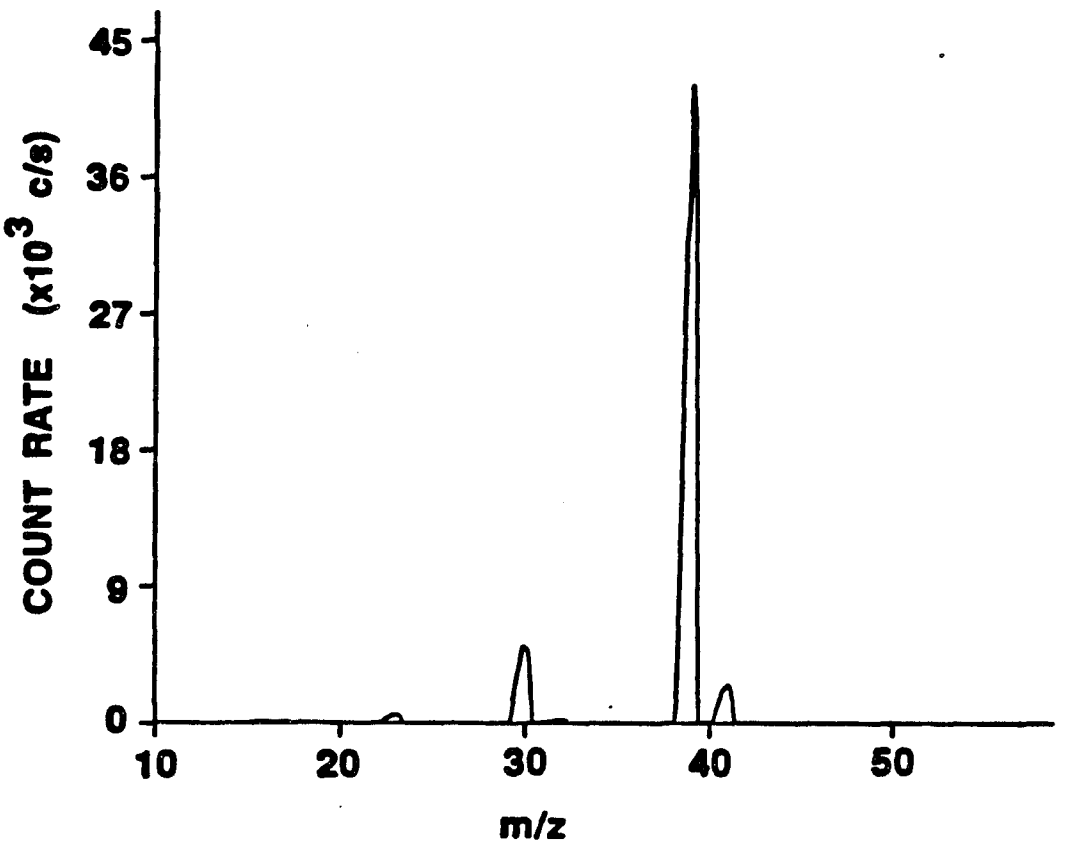

Figure 2. Mass spectrum obtained from a potassium solution (10 mg L^{-1}) in deionized distilled water

Isotope Ratios and Calibration Curves

Isotope ratio data for various solutions containing only K are listed in Table 3. The precision (0.6% RSD or better) was comparable to that normally seen in ICP-MS for a large isotope ratio. Choice of solvent (deionized water or 1% HNO_3) did not affect either the precision or the mean values. The certified value for the ratio $^{39}K/^{41}K$ in the standard reference material was 13.86, i.e., about 9% lower than the value of 15.05 obtained if the means shown in Table 3 were averaged. This bias effect was rather more extensive than usually seen in ICP-MS, as ratios for other isotopes two m/z units apart have been shown to differ systematically from the accepted values by 2 - 10% relative (1,23,24). The voltage applied to the photon stop (S2) was selected to maximize the K^+ signal at the plasma operating conditions chosen. In fact, the determined isotope ratio did depend on both ion lens voltages and plasma operating conditions, as might be expected because K^+ was the dominant ion in the spectrum. By changing the voltage on the photon stop, the ratio $^{39}K/^{41}K$ could be reduced to as low as 14.65 (~ 1.0% RSD) at the cost of a ~ 10% loss of K^+ signal. These observations show that analysis of standards of known isotopic composition and careful control of operating parameters are necessary, as is generally the case for isotope ratio measurements by ICP-MS under normal conditions.

Calibration curves for the two main potassium isotopes are shown in Figure 3. The slopes of both curves changed at about 10 mg L^{-1}. This transition was likely due to the major component of the ion beam changing from NO^+ to K^+ as potassium concentration increased, as shown

Table 3. Potassium isotope ratio measurements

Potassium concentration (mg L^{-1})	Solvent	Determined $^{39}K/^{41}K$ Mean	RSD (%)
1	DDW[a]	15.12	0.6
5	DDW	14.92	0.3
10	DDW	15.06	0.1
20	DDW	15.06	0.5
50	DDW	15.17	0.6
5	1% HNO_3 in DDW	14.95	0.5
10	1% HNO_3 in DDW	15.01	0.3
20	1% HNO_3 in DDW	15.10	0.5

[a]Deionized distilled water.

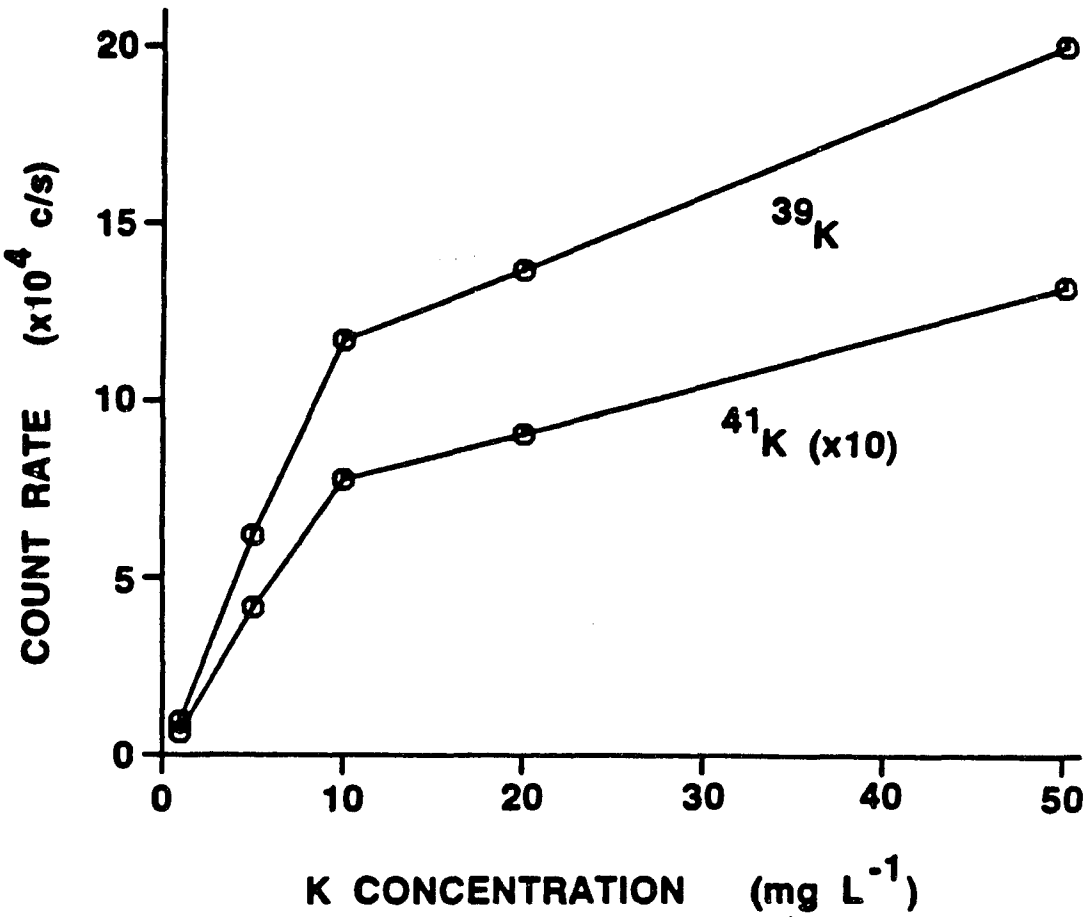

Figure 3. Calibration curves obtained for potassium solutions. The count rates for the less abundant isotope (^{41}K) have been multiplied by 10

in Figure 2. However, the determined isotope ratio (Table 3) did not depend systematically on the potassium concentration within the uncertainties of the measurements. Thus, the nonlinearity of the calibration curves should not present a problem for isotope ratio measurements.

Interferences

The low overall abundance of background ions (Figures 1 and 2) and the curved calibration plots (Figure 3) led to the suspicion that matrix effects (25-28), sometimes also called ionization interferences (29,30), would be substantial. Sodium was chosen as a likely matrix element because it is generally present in biological materials at levels comparable to potassium. The effect of sodium on potassium isotope ratios and count rate is shown in Table 4. The determined isotope ratios decreased gradually as the concentration of sodium increased. In general, the precision was slightly worse than if the solution contained only K (Table 3) and also got worse as sodium concentration increased. Sodium at 25 mg L^{-1} induced almost 50% loss in the count rate for $^{39}K^{+}$, but the sensitivity did not change much further when more sodium was added. It is interesting to note that a calibration curve for potassium plotted from the last three entries (i.e., when the sodium concentration was 100 mg L^{-1}) was linear (correlation coefficient = 0.9999) with an intercept close to the origin. In these cases, the ion beam was dominated by Na^{+}. Changing the potassium concentration from 5 to 20 mg L^{-1} did not add sufficient K^{+} to greatly affect the total ion beam

Table 4. Effect of Na concomitant on sensitivity and isotope ratios for K

Concentrations ($mg\ L^{-1}$)		$^{39}K^+$ count rate	Determined $^{39}K/^{41}K$	
K	Na	(counts s^{-1})	Mean	RSD (%)
10	--	94600[a]	14.96	0.3
10	25	50600	14.92	0.6
10	50	50100	14.85	0.7
10	75	51500	14.61	0.8
10	100	54300	14.59	0.8
5	100	26700	14.59	0.5
20	100	110000	14.67	0.9

[a]Rounded to three significant figures.

composition, so the response for K^+ varied linearly with potassium concentration. This observation, when compared to the non-linear calibration curves for K alone (Figure 3), corroborates the contention of Gillson et al. that non-spectroscopic matrix interferences in ICP-MS are caused largely by space charge effects in the ion beam, and that these vary as the ion beam composition varies (31).

The data in Table 4 indicate that sodium should be either removed or its concentration controlled if potassium isotope ratios are to be measured. Other concomitants probably also affect the potassium isotope ratios and should be removed or their concentrations controlled as well. Straightforward chemical methods, which were developed for gravimetric determination of potassium (32), are available for such separations. At present, chemical separations are generally used anyway for tracer experiments with most elements to remove interferences and to adjust the analyte concentration for optimum precision (2-5). Potassium is generally one of the most abundant metals in biological samples, so isolation of sufficient potassium should not be a problem.

Additional Observations

The signal levels in Figure 2 and the general magnitude of the precision figures in Table 3 were reproducible on four different days. The interference experiments (Table 4) were duplicated twice with essentially the same results each time.

The general concept of modifying ICP conditions to facilitate isotope ratio measurements should be valuable for other elements also.

For example, the major isotope of calcium can be readily observed at m/z = 40, and the ratio $^{40}Ca/^{44}Ca$ at natural abundance can be measured with a precision of ~ 1% RSD. "Warmer" ICP conditions that are more or less intermediate between the two sets shown in Table 1 suffice to completely remove ArO^+, freeing m/z = 56 for measurement of the major iron isotope.

Finally, a note of caution about reproducing these results on other ICP-MS instruments is appropriate. For the device used in the present work, the load coil geometry is such that there is little or no electrical discharge between the plasma and the sampling orifice. The plasma potential and ion kinetic energies are low and are largely independent of sampling position and plasma operating parameters (33-35). With some other load coil geometries, a mild secondary discharge persists, the intensity of which tends to increase as aerosol gas flow rate increases, as power decreases, and as the sampler is moved further from the load coil (36-39). In this case, as "cooler" plasma conditions are used, the intensification of the secondary discharge would keep Ar^+ and ArH^+ at substantial levels. In fact, with either of our "homemade" ICP-MS devices (37,40), we have not yet been able to attenuate Ar^+ and ArH^+ appreciably by altering the plasma parameters and sampling position. Thus, the adjusted operating conditions described herein may not be generally applicable for simplifying the background spectrum with all types of ICP-MS devices.

LITERATURE CITED

1. Ting, B. T. G.; Janghorbani, M. Spectrochim. Acta, 1987, 42B, 21.
2. Serfass, R.E.; Thompson, J. J.; Houk, R. S. Anal. Chim. Acta, 1986, 188, 73.
3. Serfass, R.E.; Lindberg, G. L.; Olivares, J. A.; Houk, R. S. Proc. Soc. Exp. Biol. Medicine, October 1987, 186, 113.
4. Janghorbani, M.; Ting, B. T. G.; Formon, S. J. Am. J. Hemat. 1986, 21, 277.
5. Ting, B. T. G.; Janghorbani, M. Anal. Chem. 1986, 58, 1334.
6. Dean, J. R.; Ebdon, L.; Massey, R. J. Anal. Atomic Spectrom. 1987, 2, 369.
7. Janghorbani, M. University of Chicago, Chicago, Illinois; Serfass, R. E. Iowa State University, Ames, Iowa, Personal communication, 1987.
8. Wilson, D. A.; Vickers, G. H.; Hieftje, G. M. Anal. Chem. 1987, 59, 1664.
9. Satzger, R. D.; Fricke, F. L.; Brown, P. G.; Caruso, J. A. Spectrochim. Acta, 1987, 42B, 705.
10. Satzger, R. D.; Fricke, F. L.; Brown, P. G.; Davidson, T. M.; Caruso, J. A. XXV Coll. Spectroscopium Int., Toronto, Ontario, 1987 Paper No. F7.7.
11. Montaser, A.; Chan, S.-K.; Kopenaal, D. W. Anal. Chem. 1987, 59, 1240.
12. Barnes, R. M.; Meyer, G. A. Anal. Chem. 1980, 52, 1522.
13. Meyer, G. A.; Thompson, M. D. Spectrochim. Acta, 1984, 40B, 195.

14. Houk, R. S. Anal. Chem. 1986, 58, 97A.

15. Tan, S. H.; Horlick, G. Appl. Spectrosc. 1986, 40, 445.

16. Houk, R. S.; Thompson, J. J. Mass Spectrom. Reviews, 1988, accepted.

17. Olson, K. W.; Haas, W. J., Jr.; Fassel, V. A. Anal. Chem. 1977, 49 632.

18. Fassel, V. A.; Bear, B. R. Spectrochim. Acta, 1986, 41B, 1089.

19. Vaughan, M. A.; Horlick, G.; Tan, S. H. J. Anal. Atomic Spectrom. 1987, 2, 765.

20. Knewstubb, P. F. "Mass Spectrometry and Ion-Molecule Reactions;" Cambridge University: London, 1969.

21. Douglas, D. J.; Quan, E. S. K.; Smith, R. G. Spectrochim. Acta, 1986, 41B, 39.

22. Gray, A. L. Dynamic Mass Spectrom. 1975, 4, 153.

23. Russ, G. P., III; Bazan, J. M.; Date, A. R. Anal. Chem. 1987, 59, 984.

24. Russ, G. P., III; Bazan, J. M. Spectrochim. Acta, 1987, 42B, 49.

25. Tan, S. H.; Horlick, G. J. Anal. Atomic Spectrom. 1987, 2, 745.

26. Beauchemin, D.: McLaren, J. W.; Berman, S. S. Spectrochim. Acta, 1987, 42B, 467.

27. Gregoire, D. C. Spectrochim. Acta, 1987, 42B, 895.

28. Kawaguchi, H.; Tanaka, T.; Nakamura, T.; Morishita, M.; Mizuiki, A. Anal. Sciences, 1987, 3, 305.

29. Olivares, J. A.; Houk, R. S. Anal. Chem. 1986, 58, 20.

30. Thompson, J. J.; Houk, R. S. Appl. Spectrosc. 1987, 41, 801.

31. Gillson, G. R.; Douglas, D. J.; Fulford, J. E.; Halligan, K. W.; Tanner, S. D. Anal. Chem. 1988, accepted.

32. Kolthoff, I. M.; Sandell, E. B.; Meehan, E. J.; Bruckenstein, S. Quantitative Chemical Analysis, 4th ed. Macmillan: London, 1969, p. 664.

33. Douglas, D. J.; French, J. B. Spectrochim. Acta, 1986, 41B, 197.

34. Fulford, J. E.; Douglas, D. J. Appl. Spectrosc. 1986, 40, 971.

35. Houk, R. S.; Schoer, J. K.; Crain, J. S. J. Anal. Atomic Spectrom. 1987, 2, 283.

36. Olivares, J. A.; Houk, R. S. Appl. Spectrosc. 1985, 39, 1070.

37. Olivares, J. A.; Houk, R. S. Anal. Chem. 1985, 57, 2674.

38. Gray, A. L.; Houk, R. S.; Williams, J. C. J. Anal. Atomic Spectrom. 1987, 2, 13.

39. Zhu, G.; Browner, R. F. Appl. Spectrosc. 1987, 41, 349.

40. Huang, L.-Q.; Jiang, S.-J.; Houk, R. S. Anal. Chem. 1987, 59, 2316.

SUMMARY AND FUTURE RESEARCH

This thesis has primarily described several alternative sample introduction methods for ICP-MS. We have demonstrated that arc nebulization is an alternative way for introducing solid samples directly into ICPs when sample dissolution is not feasible. This nebulization technique is a useful adjunct to ICP-MS for analysis of metals as well as powders. More research is warranted to demonstrate the reliability and general applicability of arc nebulization.

We also demonstrated that ICP-MS could be used as an element and isotope selective detector for liquid chromatography (LC) and flow injection (FI) sample introduction. The advantages of low detection limits, multielement capability, and the ability to measure isotope ratios on eluting peaks, which ICP-MS offers as an LC detector, has been demonstrated in this thesis by several experiments. In section three, a simple liquid chromatographic procedure to remove some spectral interferences and matrix effects was described. In section four, we demonstrated that ICP-MS is a sensitive and selective detector for LC separation of some nonmetallic compounds.

There are several important problems still facing LC-ICP-MS researchers. First, the basic criterion for a successful LC-ICP experiment is efficient interface performance. Currently, a reliable LC-ICP interface with low dead volume and high analyte mass transport efficiency is still needed. Second, it is usually necessary to use organic solvents in the mobile phase. The organic solvent generally reduces the ionization properties of the plasma significantly.

Significant changes in droplet size or solvent loading reaching the plasma affect both accuracy and reproducibility. From this standpoint, the nebulization efficiency should be independent of solvent composition. Furthermore, gradient elution technique is normally employed to separate a complicated mixture with LC. It is still questionable whether baseline drift can be avoided when the organic solvent content of the mobile phase changes during a concentration program.

It is possible to overcome the negative effect of increased solvent transport to the plasma. Oxygen may be added to the plasma to oxidize the organic species present. Excess solvent vapor may be removed before aerosol is introduced to the plasma with either a cooled spray chamber or a condenser. Nevertheless, more experiments have to be done before we can conclude that ICP-MS will be an universal detector for metal species separated by LC.

Finally, very little is mentioned in the literature about the applications of LC to "real" samples. In any real sample analysis, sample introduction is an extension of sample preparation. It is easy to see the problem in the sample preparation step: a real sample must be dissolved without changing the oxidation state or chemical form of the analyte element(s). In some cases, sample preparation may be hold the key for a successful element speciation measurement.

Many of the devices presently proposed as alternatives to liquid sample introduction offer great promise for specific applications; many more sample introduction techniques will be adapted for ICP-MS. However, to achieve widespread use, they will have to demonstrate the

reliability, general applicability, and the ease of use that liquid sample introduction currently enjoys.

ACKNOWLEDGEMENTS

In many ways, the completion of this thesis was a group effort; many people have provided the emotional and technical support required for me to carry out the work. Thanks go to Dr. R. S. Houk for his direction and assistance in the conduction of the research and in the critical evaluation of this thesis. The various collaborators Dr. V. A. Fassel, Mr. E. L. DeKalb, Dr. J. S. Fritz, Margo Palmieri made much of this research possible, and I thank them. I would also like to thank the past and present members of Dr. Houk's research group for all the encouragement and assistance provided. I am also grateful to Eldon Ness in the machine shop for his skillful help in making the sampler and skimmer and numerous odd jobs and to Harold Hall for providing several ICP torches and other pieces of glassware. Finally I thank my parents for their constant encouragement and support. Without them this thesis would never have been written.

This work was performed at Ames Laboratory under contract No. W-7405-eng-82 with the U. S. Department of Energy. The United States government has assigned the DOE Report number IS-T 1357 to this thesis.